Transmit Power Optimization and Feasibility Analysis of Self-backhauling Full-Duplex Radio Access Systems

Dani Korpi, *Member, IEEE,* Taneli Riihonen, *Member, IEEE,* Ashutosh Sabharwal, *Fellow, IEEE,* and Mikko Valkama, *Senior Member, IEEE*

***Abstract*—We analyze an inband full-duplex access node that is serving mobile users while simultaneously connecting to a core network over a wireless backhaul link, utilizing the same frequency band for all communication tasks. Such wireless self-backhauling is an intriguing option for the next generation wireless systems since a wired backhaul connection might not be economically viable if the access nodes are deployed densely. In particular, we derive the optimal transmit power allocation for such a system in closed form under Quality-of-Service (QoS) requirements, which are defined in terms of the minimum data rates for each mobile user. For comparison, the optimal transmit power allocation is solved also for two reference scenarios: a purely half-duplex access node, and a relay-type full-duplex access node. Based on the obtained expressions for the optimal transmit powers, we then show that the systems utilizing a full-duplex capable access node have a fundamental feasibility boundary, meaning that there are circumstances under which the QoS requirements cannot be fulfilled using finite transmit powers. This fundamental feasibility boundary is also derived in closed form. The feasibility boundaries and optimal transmit powers are then numerically evaluated in order to compare the different communication schemes. In general, utilizing the purely full-duplex access node results in the lowest transmit powers for all the communicating parties, although there are some network geometries under which such a system is not capable of reaching the required minimum data rates. In addition, the numerical results indicate that a full-duplex capable access node is best suited for relatively small cells.**

***Index Terms*—Self-backhauling, full-duplex wireless, massive MIMO, transmit power optimization.**

I. Introduction

WIRELESS inband full-duplex communications is widely considered to be one of the key enabling technologies in achieving the required throughput gains of the future 5G networks. Its basic idea is to allow a radio to transmit and receive data signals simultaneously using the same center frequency, and hence it has the capability to double the spectral efficiency of the existing systems as long as its full potential can be harnessed properly [1]–[5]. Many real-world demonstrations of inband full-duplex radios have already been developed by various research groups, which indicates that the concept is indeed feasible [1], [5]–[8]. In addition, the framework and theoretical boundaries of inband full-duplex radios have been studied extensively in the recent years [2], [9]–[15].

In terms of a practical implementation, the fundamental issue for inband full-duplex devices is the coupling of the own transmit signal to the receiver. In particular, since the transmission and reception occur simultaneously over the same frequency channel, the transceiver will inherently receive its own transmit signal. What makes this especially problematic is the extremely high power level of the own transmission at this stage, which means that it will completely drown out the intended received signal. This phenomenon is typically referred to as self-interference (SI), and reducing its effect has been one of the main research areas in this field. The various proposed SI cancellation solutions [7], [16]–[20] and actual implementations and measurements already show that solving the problem of SI is not far from reality [1], [6]–[8], [20], [21].

In addition to SI cancellation, a large portion of the research has also focused on how to best make use of the full-duplex capability on a network level [4], [22]–[24]. This is a tedious issue since in many applications the traffic requirements are highly asymmetric between the two communication directions, such as in mobile networks [25]. Because the inband full-duplex principle requires completely symmetric traffic to realize the doubling of spectral efficiency at radio link level, this will compromise the potential throughput gains it can provide in practice. Thus, more advanced schemes are likely needed in order to realize the full potential of inband full-duplex radios in practical network scenarios. One such option is employing a full-duplex access node (AN) in an otherwise legacy half-duplex mobile cell [4], [23], [24], [26], thereby allowing the AN to simultaneously serve the uplink (UL) and the downlink (DL) using the very same frequency resources. With proper multiplexing and active scheduling, such a scheme enables the AN to fully exploit its full-duplex capability in both directions [4].

In this paper, the above type of a scheme will be analyzed and developed further under a scenario where installing wired backhaul links for all the cells is not feasible. This means that

Manuscript received February 20, 2017; revised September 14, 2017 and January 19, 2018; accepted March 25, 2018. This work was supported in part by the Academy of Finland (under the projects #301820, #304147, and #310991), in part by the Finnish Funding Agency for Technology and Innovation (Tekes, under the TAKE-5 project), in part by Tampere University of Technology Graduate School, in part by Nokia Foundation, in part by Tuula and Yrjö Neuvo Research Fund, and in part by Emil Aaltonen Foundation. *(Corresponding author: Dani Korpi.)*

D. Korpi, T. Riihonen, and M. Valkama are with the Laboratory of Electronics and Communications Engineering, Tampere University of Technology, Tampere, Finland, e-mail: dani.korpi@tut.fi.

A. Sabharwal is with the Department of Electrical and Computer Engineering, Rice University, Houston, TX 77005, USA.

Color versions of one or more of the figures in this paper are available online at http://ieeexplore.ieee.org

Digital Object Identifier 10.1109/TWC.2018.XXXXXXX

wireless *self-backhauling*, where the same frequency band is also used to backhaul the UL and DL data, is required [24], [27]–[33]. This type of a situation can occur, for instance, due to densely deployed cells, a probable scenario in the future 5G networks [34], [35]. Hence, in addition to communicating with the user equipments (UEs), also the backhaul data is transferred inband with a wireless point-to-point link between the AN and a so-called backhaul node (BN). The BN then further connects to the actual core network using either a wired or a wireless link. As the self-backhauling is performed on the same frequency band as the DL and UL data transfer, no additional spectral resources are needed, which further improves the applicability of such a solution.

This type of inband self-backhauling has been also investigated in the earlier literature. Therein, most works have considered a relay-type AN that is directly forwarding the signals transmitted by the UL UEs to the BN, or vice versa [27]–[30], [32], [36], [37]. The reason for this is likely the fact that such a relay-type AN is more or less directly compatible with the existing networks, as it would essentially just extend the range of the BN or macro base station (BS). In particular, in [27], [36], the power control of such a relay-type AN is investigated, and the performance of both half-duplex and full-duplex operation modes is then compared. The findings obtained in [27], where the transmit powers are numerically optimized, indicate that the full-duplex AN can obtain higher throughputs than the corresponding half-duplex system. The same conclusion is reached in [36], where the spectral efficiency of a similar system is maximized by solving the optimal power allocation for both full-duplex and half-duplex ANs, with the power allocation of the former being solved using an iterative algorithm.

Moreover, the effect of radio resource management (RRM) on the performance of the relay-type full-duplex AN is investigated in [28], where the resulting solution is shown to outperform the half-duplex benchmark scheme. The work in [29], on the other hand, investigates different beamforming solutions for a BN with massive antenna arrays, although no full-duplex operation is assumed in any of the nodes therein. The DL coverage of a relay-type self-backhauling AN is then analyzed in [30], [37]. The findings in [37] indicate that, while the throughput of the network with full-duplex-capable ANs is almost doubled in comparison to the half-duplex systems, the increased interference levels result in a somewhat smaller coverage. The results obtained in [30] suggest, on the other hand, that on a network level it may be better to have also some ANs that perform the self-backhauling on a different frequency band, in order to reduce the interference levels. The work in [32] analyzes the throughput and outage probability of a relay-type full-duplex AN under an antenna selection scheme where individual transmit and receive antennas are chosen in the AN based on a given criterion. Again, the full-duplex AN is shown to usually outperform the corresponding half-duplex AN.

All in all, even though different inband self-backhauling solutions for small cells have been investigated in the earlier literature, none of the above works have considered a scenario where also the UL and DL transmissions are performed simultaneously on the same center frequency. Considering the promising findings regarding the relay-type scenario where the DL and UL are separated either in time or in frequency, this means that the purely full-duplex scheme analyzed in this article is an intriguing option for further improving the spectral efficiency of these types of networks. Furthermore, to properly evaluate the full-duplex self-backhauling solution for the AN, its performance is compared to two reference schemes, one of which relies on traditional half-duplex communication while in the other the AN acts as a one-directional full-duplex relay. The latter reference scheme corresponds to the solution mostly investigated in the earlier works.

In addition, in this article it is also assumed that the AN has large arrays of antennas at its disposal. Therefore, in the full-duplex solution, the same time-frequency resource can be used for all the individual UL and DL transmissions, as well as for the wireless backhaul link, since such massive antenna arrays allow for efficient beamforming, which can be used to prevent the interference between the various spatial streams [24], [30], [33]. The massive arrays also facilitate efficient attenuation of the SI by zero-forcing (ZF) beamforming [9], [38]. Namely, the transmit signals will be precoded such that nulls are formed in the positions of all the receive antennas, which will significantly decrease the SI power coupled back to the receivers. To suppress the residual SI remaining after the ZF procedure, additional SI cancellation can also be performed, e.g., in the digital domain [3], [6], [8], [17].

The different communication schemes are then analyzed under a scenario where a minimum Quality-of-Service (QoS) requirement is given for each UE, defined in terms of minimum DL and UL data rates. This definition ensures uniform QoS for all the UEs, which makes it a reasonable choice. The problem is then to determine the minimum transmit powers for each communicating party under the constraint that each UE achieves the minimum required data rate. Furthermore, since wireless self-backhauling is assumed, the AN and the BN must also allocate some transmit power for the backhaul link to ensure sufficient backhauling capability. A similar system was considered by the authors already in [33], where the sum-rate was optimized under a greatly simplified system model, while the transmit power minimization under QoS constraints was preliminarily considered in [24]. The current article completes and archives our research work in the most comprehensive form under a generic setting by presenting closed-form solutions for the optimal transmit powers in three different communication schemes: a full-duplex scheme, a half-duplex scheme, and a hybrid relay scheme. To the best of our knowledge, this is something that has not been solved before for any self-backhauling radio access system.

The major contributions of this paper can be detailed as follows:

- We derive closed-form solutions for the optimal transmit powers of all the considered communication schemes that fulfill the QoS requirements.
- We show that the full-duplex and hybrid relay schemes cannot always fulfill the QoS requirements, even if the transmit powers tend towards infinity. In other words, these two schemes are feasible only under some circumstances,

meaning that there is a fundamental limit for the data rates that they can achieve. The condition for this is derived in closed form, while accurate approximations for the feasibility boundary are also provided.
- We provide extensive numerical results to illustrate different aspects of the considered communication schemes. In particular, the numerical results show that in most cases the full-duplex scheme is indeed the most transmit power efficient solution. However, the results also indicate that the schemes utilizing a full-duplex capable AN are fundamentally limited to relatively small cell sizes.

The rest of this article is organized as follows. The system model is first presented in Section II, alongside with the achievable DL and UL data rate expressions of the three different communication schemes. The optimal QoS-fulfilling transmit powers are then derived in Section III. After this, the feasibility of the full-duplex and hybrid relay schemes is investigated in Section IV, the feasibility boundaries being derived in closed form. The numerical results are then given and analyzed in Section V, while the conclusions are drawn in Section VI.

II. System Model, Communication Schemes, and Sum-Rate Expressions

Let us consider a wireless cell with a large-array AN that is communicating with a multiple-input and multiple-output (MIMO) BN and half-duplex single-antenna UEs, the UEs being further divided into UL and DL UEs. The AN is assumed to have N_t transmit and N_r receive antennas, while the amount of transmitted and received signal streams is assumed to be significantly lower. Moreover, the same antenna arrays are used for serving the DL and UL UEs as well as for communicating with the BN, the AN forwarding the data between the UEs and the BN in a decode-and-forward manner. As for the number of BN antennas, the analysis can be interpreted such that the number of backhaul signal streams in either direction is equal to the number of corresponding BN antennas. Three different communication schemes are analyzed in this article, each of them depicted in Fig. 1. Below, we describe the different communication schemes in detail, and also derive the expressions of the achievable data rates for each scheme. These can then be used in determining the optimal transmit power allocations.

A. Full-Duplex Scheme

In the full-duplex scheme, the AN transmits signals simultaneously to the BN and to the DL UEs while also receiving signals from the UL UEs and the BN, all of the transmissions occurring on the same center frequency. Consequently, both the AN and the BN must be full-duplex capable, while the UEs are legacy half-duplex devices, as already mentioned. This type of a full-duplex system suffers from the SI, the IUI between the UL and the DL UEs, as well as from the interference between the BN and the UEs. Even though there are also advanced methods for attenuating the UL-to-DL IUI [39]–[41], in this work we assume that its power level is only affected by the transmit power of the UL UEs and the path losses between the UL and DL UEs.

Denoting the number of DL UEs by D and the number of transmitted backhaul signal streams by M_t^B, the overall stacked spatial signal received by the UEs and the BN can be represented as a vector, whose first D elements contain the samples received by the DL UEs, while the last M_t^B elements contain the samples received by the BN (consisting of the parallel streams of backhauled UL data). This total received signal vector can be written as follows:

$$\mathbf{y} = \mathbf{L}_\mathrm{t}\mathbf{H}_\mathrm{t}\mathbf{x} + \mathbf{z}, \tag{1}$$

where $\mathbf{L}_\mathrm{t} = \mathrm{diag}\left(\sqrt{L_1^\mathrm{d}}, \ldots, \sqrt{L_D^\mathrm{d}}, \ldots, \sqrt{L_\mathrm{B}}, \ldots, \sqrt{L_\mathrm{B}}\right)$ is a $(D + M_\mathrm{t}^\mathrm{B}) \times (D + M_\mathrm{t}^\mathrm{B})$ diagonal matrix, L_i^d is the path loss normalized fading variance between the AN and the ith DL UE, L_B is the path loss normalized fading variance between the AN and the BN, $\mathbf{H}_\mathrm{t} \in \mathbb{C}^{(D+M_\mathrm{t}^\mathrm{B})\times N_\mathrm{t}}$ is the normalized channel matrix between the AN and all the intended receivers, $\mathbf{x} \in \mathbb{C}^{N_\mathrm{t}\times 1}$ is the transmit signal of the AN and $\mathbf{z} \in \mathbb{C}^{(D+M_\mathrm{t}^\mathrm{B})\times 1}$ represents the different noise and interference sources. In this article, Rayleigh fading between all communicating parties is assumed, which means that the entries of $\mathbf{H}_\mathrm{t}$ are independent and identically distributed (i.i.d.) zero-mean complex Gaussian random variables with unit variance. In the continuation, to simplify the literary presentation, the path loss normalized fading variances are simply referred to as path losses. Also note that, while the path losses between the AN and the UEs are different, the path losses of the backhaul signals are identical as they all correspond to the link between the AN and the BN.

The precoded transmit signal $\mathbf{x}$ is formed from the DL and backhaul transmit data as follows:

$$\mathbf{x} = \mathbf{W}\mathbf{\Gamma}\mathbf{q}, \tag{2}$$

where $\mathbf{W} \in \mathbb{C}^{N_\mathrm{t}\times(D+M_\mathrm{t}^\mathrm{B})}$ is the precoding matrix, $\mathbf{q} \in \mathbb{C}^{(D+M_\mathrm{t}^\mathrm{B})\times 1}$ contains all the transmit data symbols, $\mathbf{\Gamma} = \mathrm{diag}\left(\sqrt{p_1^\mathrm{d}}, \ldots, \sqrt{p_D^\mathrm{d}}, \ldots, \sqrt{P_\mathrm{u}^\mathrm{B}/M_\mathrm{t}^\mathrm{B}}, \ldots, \sqrt{P_\mathrm{u}^\mathrm{B}/M_\mathrm{t}^\mathrm{B}}\right)$ is a $(D+M_\mathrm{t}^\mathrm{B}) \times (D + M_\mathrm{t}^\mathrm{B})$ diagonal matrix, p_i^d is the transmit power allocated for the ith DL signal stream, and P_u^B is the total transmit power allocated for backhauling the UL data. The power of the data symbols is assumed to be normalized as $\mathrm{E}\left[|q_i|^2\right] = 1$ where q_i is the ith element of $\mathbf{q}$. Even though the transmitter's power amplifier–induced nonlinear distortion is typically a significant issue in full-duplex devices [3], in this analysis we are using a linear signal model for simplicity. In fact, in a massive MIMO transmitter, the powers of the individual transmitters are typically small, which somewhat alleviates the effects of the nonlinearities.

The precoding is performed using ZF beamforming since it typically performs well under high signal-to-noise ratios [42]. Assuming that also the effective SI channel experiences Rayleigh fading, the SI channel matrix between the AN transmitters and receivers can be expressed as $\mathbf{L}_\mathrm{s}\mathbf{H}_\mathrm{s} \in \mathbb{C}^{N_\mathrm{r}\times N_\mathrm{t}}$, where $\mathbf{L}_\mathrm{s}$ is a diagonal matrix containing the amounts of SI suppression between the transmitter and receiver pairs without any ZF nulling (assuming that the amounts of SI suppression are equal for all transmitter and receiver pairs) and the elements

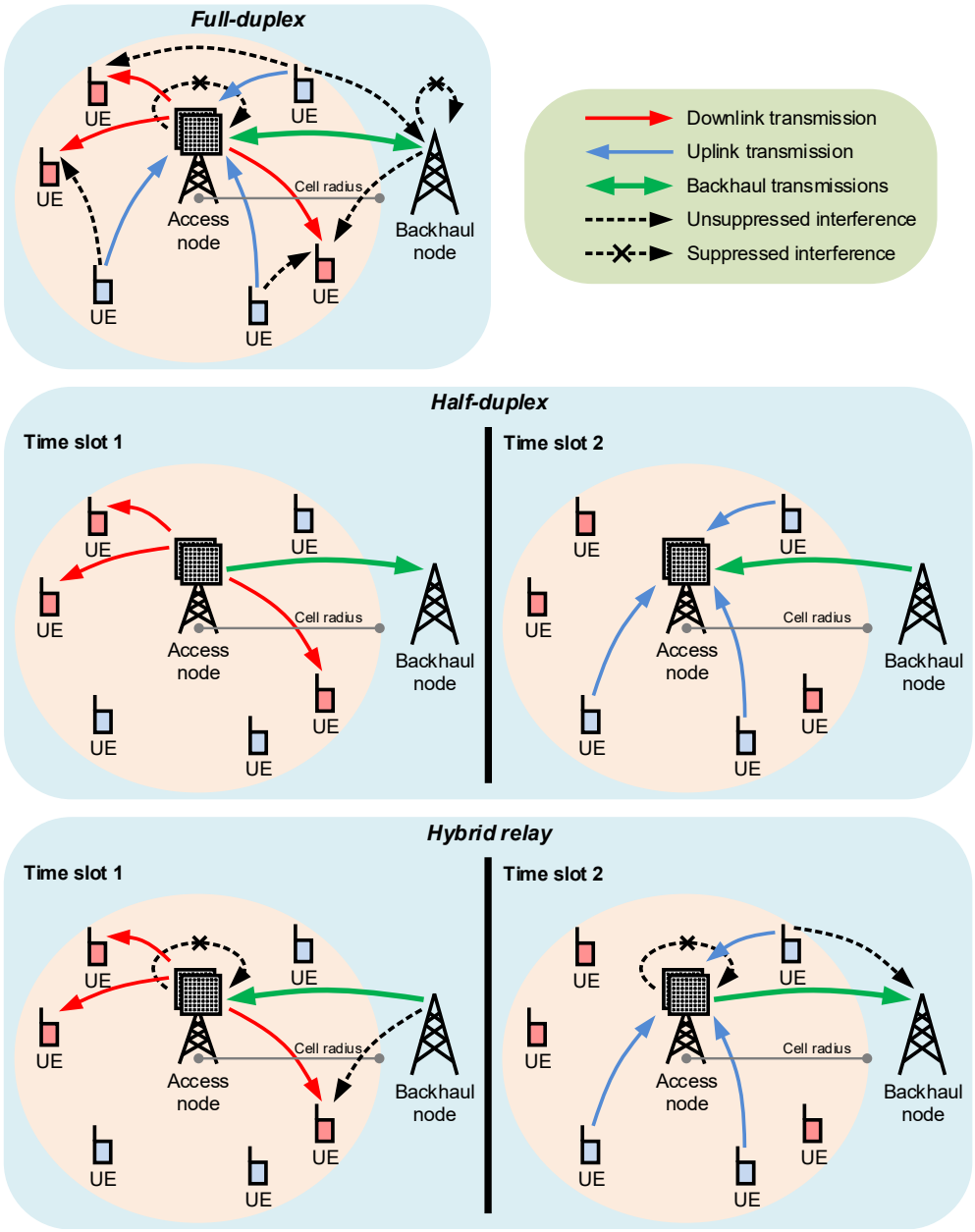

Fig. 1: An illustration of the three considered communication schemes: the *full-duplex* scheme, the *half-duplex* scheme, and the *hybrid relay* scheme.

of $\mathbf{H}_{\mathrm{s}}$ are i.i.d. zero-mean complex Gaussian random variables with unit variance. Note that assuming the SI channel to experience Rayleigh fading can be expected to be relatively accurate when there is a certain level of active SI suppression before the total received signal is decoded [1]. For the same reason, the overall SI suppression between each transmitter and receiver pair can be expected to be roughly the same, as more active SI cancellation is typically obtained in the receivers with stronger SI coupling in the antenna interface [1].

Under the condition that the AN has full knowledge of the channel state information (CSI) of the links used for data transfer (that is, the channel matrix $\mathbf{H}_{\mathrm{t}}$ is fully known) and assuming that $N_t > N_r+D+M_{\mathrm{t}}^{\mathrm{B}}$, the transmitter ZF precoding matrix in full-duplex mode can then be written as [42]

$$\mathbf{W} = \mathbf{H}^H \left(\mathbf{H}\mathbf{H}^H\right)^{-1} \mathbf{\Lambda}, \tag{3}$$

where $\mathbf{H}^H = \begin{bmatrix} \mathbf{H}_{\mathrm{t}}^H & \widehat{\mathbf{H}}_{\mathrm{s}}^H \end{bmatrix}$, $\widehat{\mathbf{H}}_{\mathrm{s}}$ is an imperfect estimate of the effective SI coupling channel, and $\mathbf{\Lambda} \in \mathbb{C}^{(D+M_{\mathrm{t}}^{\mathrm{B}}+N_{\mathrm{r}})\times(D+M_{\mathrm{t}}^{\mathrm{B}})}$ is a non-square diagonal normalization matrix containing the normalization factor $\sqrt{N_{\mathrm{t}} - D - M_{\mathrm{t}}^{\mathrm{B}} - N_{\mathrm{r}}}$ in each diagonal entry [38], [42]. Moreover, $(\cdot)^H$ denotes the Hermitian transpose. The purpose of the normalization matrix is simply to ensure that precoding does not affect the expected effective powers of the data symbols.

It should be noted that assuming the AN to have full knowledge of the CSI of the data transfer links is obviously not fully practical, but it allows the derivation of analytical data rate expressions that provide information about the ultimate performance limits of the considered system. Namely, this assumption means that, apart from SI, none of the signals received or transmitted by the AN interfere with each other,

TABLE I: The most important symbols used in the article.

Variable	Definition
N_t / N_r	Number of transmit/receive antennas in the AN
$M_{\mathrm{t}}^{\mathrm{B}}$ / $M_{\mathrm{r}}^{\mathrm{B}}$	Number of backhaul signal streams transmitted/received by the AN
D / U	Number of DL/UL UEs in the cell
$\Lambda_{\mathrm{t}}^{\mathrm{X}}$ / $\Lambda_{\mathrm{r}}^{\mathrm{X}}$	The degrees-of-freedom of the AN transmitter/receiver, $\mathrm{X} = \{\mathrm{FD}, \mathrm{HD}, \mathrm{RL}\}$
L_i^{d} / L_j^{u}	Path loss between the AN and the ith DL / jth UL UE
L_{ij}^{ud}	Path loss between the ith DL and the jth UL UE
L_i^{Bd} / L_j^{Bu}	Path loss between the BN and the ith DL / jth UL UE
L_{B}	Path loss between the AN and the BN
σ_{n}^2	Noise floor in all the receivers
$\alpha_{\mathrm{AN}}/\alpha_{\mathrm{BN}}$	Amount of SI cancellation in the AN/BN
p_i^{d}	Transmit power used for the ith DL signal stream
p_j^{u}	Transmit power of the jth UL UE
$P_{\mathrm{d}}^{\mathrm{B}}$	Total amount of transmit power used by the BN
$P_{\mathrm{u}}^{\mathrm{B}}$	Total amount of transmit power allocated for self-backhauling in the AN
η	Proportion of time spent in the DL time slot (in the half-duplex and hybrid relay schemes)
ρ_{d} / ρ_{u}	DL/UL rate requirement of an individual UE

representing a best-case scenario in this respect. Nevertheless, the effect of residual SI is still considered in the system, as no full knowledge of the effective SI coupling channel is assumed. Furthermore, in order to simplify the system models and derivations, only the beamforming performed by the AN is explicitly considered, meaning that analysis of any potential spatial domain processing in the other nodes is omitted.

Now, we can rewrite the signals received by the DL UEs and the BN as

$$\mathbf{y} = \mathbf{L}_{\mathrm{t}}\mathbf{H}_{\mathrm{t}}\mathbf{x} + \mathbf{z} = \mathbf{L}_{\mathrm{t}}\mathbf{H}_{\mathrm{t}}\mathbf{W}\boldsymbol{\Gamma}\mathbf{q} + \mathbf{z} = \mathbf{L}_{\mathrm{t}}\widetilde{\boldsymbol{\Lambda}}\boldsymbol{\Gamma}\mathbf{q} + \mathbf{z}, \quad (4)$$

where $\widetilde{\boldsymbol{\Lambda}} \in \mathbb{C}^{(D+M_{\mathrm{t}}^{\mathrm{B}})\times(D+M_{\mathrm{t}}^{\mathrm{B}})}$ denotes $\boldsymbol{\Lambda}$ with all the zero rows removed. To express the individual received data streams, (4) can alternatively be written component wise using the elements of the various vectors and matrices. Then, we get

$$y_i = \begin{cases} \sqrt{L_i^{\mathrm{d}}\left(N_{\mathrm{t}} - D - M_{\mathrm{t}}^{\mathrm{B}} - N_r\right)p_i^{\mathrm{d}}}q_i + z_i,\ i = 1,\ldots,D \\ \sqrt{L_{\mathrm{B}}(N_{\mathrm{t}} - D - M_{\mathrm{t}}^{\mathrm{B}} - N_r)\frac{P_{\mathrm{u}}^{\mathrm{B}}}{M_{\mathrm{t}}^{\mathrm{B}}}}q_i + z_i,\ i = D+1,\ldots,D+M_{\mathrm{t}}^{\mathrm{B}} \end{cases} \quad (5)$$

Stemming from (5) and assuming a large transmit antenna array [38], [42], the signal-to-interference-plus-noise ratio (SINR) of the ith DL signal can then be expressed as follows for the full-duplex scheme:

$$\begin{aligned} \mathit{SINR}_i^{\mathrm{d,FD}} &= \frac{\mathrm{E}\left[\left|y_i - z_i\right|^2\right]}{\mathrm{E}\left[\left|z_i\right|^2\right]} \\ &= \frac{\mathrm{E}\left[\left|\sqrt{L_i^{\mathrm{d}}\left(N_{\mathrm{t}} - D - M_{\mathrm{t}}^{\mathrm{B}} - N_{\mathrm{r}}\right)p_i^{\mathrm{d}}}q_i\right|^2\right]}{\mathrm{E}\left[\left|z_i\right|^2\right]} \\ &= \frac{\Lambda_{\mathrm{t}}^{\mathrm{FD}}L_i^{\mathrm{d}}p_i^{\mathrm{d}}}{\sigma_{\mathrm{n}}^2 + L_i^{\mathrm{Bd}}P_{\mathrm{d}}^{\mathrm{B}} + \sum_{j=1}^{U}L_{ij}^{\mathrm{ud}}p_j^{\mathrm{u}}}, \quad i = 1,\ldots,D \end{aligned} \quad (6)$$

where the power of the noise-plus-interference term z_i has been expanded to reflect the various components, $\Lambda_{\mathrm{t}}^{\mathrm{FD}} = N_{\mathrm{t}} - N_{\mathrm{r}} - D - M_{\mathrm{t}}^{\mathrm{B}}$, and the rest of the symbols are as defined in Table I. To further illustrate the many symbols and parameters used throughout this work, Fig. 2 provides also a visual depiction of their meaning within the considered system.

Similarly, the SINR of the backhaul signal streams transmitted by the AN, used for backhauling the UL data, can be written as

$$\mathit{SINR}_{\mathrm{B}}^{\mathrm{u,FD}} = \frac{\Lambda_{\mathrm{t}}^{\mathrm{FD}}L_{\mathrm{B}}P_{\mathrm{u}}^{\mathrm{B}}}{M_{\mathrm{t}}^{\mathrm{B}}\left(\sigma_{\mathrm{n}}^2 + \alpha_{\mathrm{BN}}P_{\mathrm{d}}^{\mathrm{B}} + \sum_{j=1}^{U}L_j^{\mathrm{Bu}}p_j^{\mathrm{u}}\right)}, \quad (7)$$

with the symbols again defined in Table I and illustrated in Fig. 2.

The SINRs of the signals *received* by the AN can be derived in an essentially similar manner as those of the transmit signals (cf. [38]), and hence their detailed derivation is omitted for brevity. In particular, the SINR of the jth UL signal can be shown to read:

$$\mathit{SINR}_j^{\mathrm{u,FD}} = \frac{\Lambda_{\mathrm{r}}^{\mathrm{FD}}L_j^{\mathrm{u}}p_j^{\mathrm{u}}}{\sigma_{\mathrm{n}}^2 + \alpha_{\mathrm{AN}}\left(P_{\mathrm{u}}^{\mathrm{B}} + \sum_{i=1}^{D}p_i^{\mathrm{d}}\right)}, \quad j = 1,\ldots,U, \quad (8)$$

where again the symbols are as defined in Table I, and $\Lambda_{\mathrm{r}}^{\mathrm{FD}} = N_{\mathrm{r}} - U - M_{\mathrm{r}}^{\mathrm{B}}$. Correspondingly, the SINR of the backhaul signals received by the AN, backhauling the DL data, is as follows:

$$\mathit{SINR}_{\mathrm{B}}^{\mathrm{d,FD}} = \frac{\Lambda_{\mathrm{r}}^{\mathrm{FD}}L_{\mathrm{B}}P_{\mathrm{d}}^{\mathrm{B}}}{M_{\mathrm{r}}^{\mathrm{B}}\left[\sigma_{\mathrm{n}}^2 + \alpha_{\mathrm{AN}}\left(P_{\mathrm{u}}^{\mathrm{B}} + \sum_{i=1}^{D}p_i^{\mathrm{d}}\right)\right]}. \quad (9)$$

The hereby obtained SINR expressions can then be used to determine the achievable rates of the full-duplex scheme. In particular, using (6), the DL sum-rate of this communication

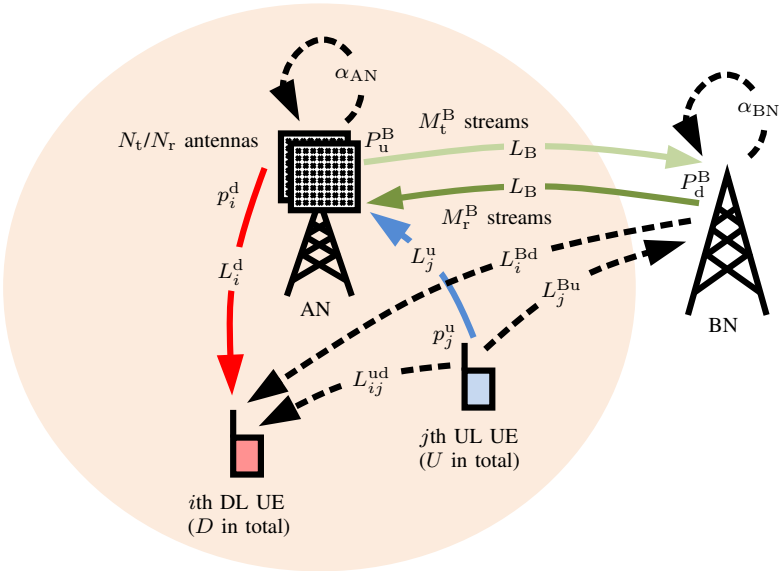

Fig. 2: An illustration depicting the relevant symbols.

scheme can be expressed as follows:

$$\begin{aligned} R^{\mathrm{d}} &= \sum_{i=1}^{D} R_i^{\mathrm{d}}, \\ R_i^{\mathrm{d}} &= \log_2\left(1 + \mathit{SINR}_i^{\mathrm{d,FD}}\right) \\ &= \log_2\left(1 + \frac{\Lambda_{\mathrm{t}}^{\mathrm{FD}} L_i^{\mathrm{d}} p_i^{\mathrm{d}}}{\sigma_{\mathrm{n}}^2 + L_i^{\mathrm{Bd}} P_{\mathrm{d}}^{\mathrm{B}} + \sum_{j=1}^{U} L_{ij}^{\mathrm{ud}} p_j^{\mathrm{u}}}\right), \end{aligned} \tag{10}$$

It can be observed that, in this communication scheme, the DL data rate is degraded by the UL-to-DL IUI and by the interference produced by the BN transmission. Similarly, using (8), the total UL data rate can be written as:

$$\begin{aligned} R^{\mathrm{u}} &= \sum_{j=1}^{U} R_j^{\mathrm{u}}, \\ R_j^{\mathrm{u}} &= \log_2\left(1 + \mathit{SINR}_j^{\mathrm{u,FD}}\right) \\ &= \log_2\left(1 + \frac{\Lambda_{\mathrm{r}}^{\mathrm{FD}} L_j^{\mathrm{u}} p_j^{\mathrm{u}}}{\sigma_{\mathrm{n}}^2 + \alpha_{\mathrm{AN}}\left(P_{\mathrm{u}}^{\mathrm{B}} + \sum_{i=1}^{D} p_i^{\mathrm{d}}\right)}\right), \end{aligned} \tag{11}$$

where the SINR is now degraded by the residual SI within the AN. Note that this work does not assume any specific SI cancellation performance since all the derivations are done for an arbitrary amount of SI suppression, consisting of passive antenna isolation, ZF beamforming at the transmit side to form nulls at the receive antennas, and other possible SI cancellation methods.

Since the AN must be capable of backhauling all the data, the backhaul data rates must also be taken into account in the analysis. With the help of (7), the data rate of the backhaul signal transmitted by the AN (for backhauling UL data) can be expressed as follows:

$$\begin{aligned} R^{\mathrm{u,B}} &= \sum_{k=1}^{M_{\mathrm{t}}^{\mathrm{B}}} \log_2\left(1 + \mathit{SINR}_{\mathrm{B}}^{\mathrm{u,FD}}\right) \\ &= M_{\mathrm{t}}^{\mathrm{B}} \log_2\left(1 + \frac{\Lambda_{\mathrm{t}}^{\mathrm{FD}} L_{\mathrm{B}} P_{\mathrm{u}}^{\mathrm{B}} / M_{\mathrm{t}}^{\mathrm{B}}}{\sigma_{\mathrm{n}}^2 + \alpha_{\mathrm{BN}} P_{\mathrm{d}}^{\mathrm{B}} + \sum_{j=1}^{U} L_j^{\mathrm{Bu}} p_j^{\mathrm{u}}}\right), \end{aligned} \tag{12}$$

which is affected by the residual SI within the BN, and also by the interference caused by the UL transmissions. In a similar fashion, using (9), the data rate of the received backhaul signal streams in the AN (for backhauling DL data) can be written as follows:

$$\begin{aligned} R^{\mathrm{d,B}} &= \sum_{l=1}^{M_{\mathrm{r}}^{\mathrm{B}}} \log_2\left(1 + \mathit{SINR}_{\mathrm{B}}^{\mathrm{d,FD}}\right) \\ &= M_{\mathrm{r}}^{\mathrm{B}} \log_2\left(1 + \frac{\Lambda_{\mathrm{r}}^{\mathrm{FD}} L_{\mathrm{B}} P_{\mathrm{d}}^{\mathrm{B}} / M_{\mathrm{r}}^{\mathrm{B}}}{\sigma_{\mathrm{n}}^2 + \alpha_{\mathrm{AN}}\left(P_{\mathrm{u}}^{\mathrm{B}} + \sum_{i=1}^{D} p_i^{\mathrm{d}}\right)}\right). \end{aligned} \tag{13}$$

The data rate of the received backhaul signals is decreased by the residual SI within the AN, similar to the UL signals. Put together, the data rate expressions in (10)–(13) can be used to determine the optimal transmit powers for the considered system under some given data rate requirements, as will be done in Section III.

B. Half-duplex Scheme

Perhaps the most obvious alternative to the aforementioned full-duplex scheme is for all the nodes to operate in half-duplex mode. This can be done by utilizing time-division duplexing (TDD) where each node within the considered system either transmits or receives at any given time, using all of the available spectrum. In terms of the analyzed AN with a wireless backhaul link, one possible TDD scheme is shown in the middle part of Fig. 1. There, the system has two different time slots: one where the AN transmits data to the BN and to the UEs, and one where

it receives data from them. As can easily be observed from Fig. 1, this type of a scheme requires only half-duplex capable nodes since none of them have to engage in simultaneous transmission and reception. This removes the problems of SI and UL-to-DL IUI at the cost of decreased spectral efficiency since the AN now requires more temporal resources to carry out the same tasks in comparison to the full-duplex scheme.

Although the detailed derivations must be omitted for brevity, the SINRs for this type of a half-duplex scheme can be obtained in a similar manner as done for the full-duplex scheme above, and the corresponding DL sum-rate of the half-duplex system can be expressed as follows:

$$\begin{aligned} R^{\mathrm{d}} &= \sum_{i=1}^{D} R_i^{\mathrm{d}}, \\ R_i^{\mathrm{d}} &= \eta \log_2 \left(1 + \mathit{SINR}_i^{\mathrm{d,HD}}\right) \\ &= \eta \log_2 \left(1 + \frac{\Lambda_{\mathrm{t}}^{\mathrm{HD}} L_i^{\mathrm{d}} p_i^{\mathrm{d}}}{\sigma_{\mathrm{n}}^2}\right), \end{aligned} \tag{14}$$

where the symbols are as defined in Table I and $\Lambda_{\mathrm{t}}^{\mathrm{HD}} = N_{\mathrm{t}} - D - M_{\mathrm{t}}^{\mathrm{B}}$. The relative lengths of the two time slots are controlled by the duplexing parameter η, which defines the proportion of time spent in the DL time slot (the relative length of the UL time slot being $1-\eta$). The corresponding UL sum-rate can then be written as:

$$\begin{aligned} R^{\mathrm{u}} &= \sum_{j=1}^{U} R_j^{\mathrm{u}}, \\ R_j^{\mathrm{u}} &= (1-\eta) \log_2 \left(1 + \mathit{SINR}_j^{\mathrm{u,HD}}\right) \\ &= (1-\eta) \log_2 \left(1 + \frac{\Lambda_{\mathrm{r}}^{\mathrm{HD}} L_j^{\mathrm{u}} p_j^{\mathrm{u}}}{\sigma_{\mathrm{n}}^2}\right), \end{aligned} \tag{15}$$

where $\Lambda_{\mathrm{r}}^{\mathrm{HD}} = N_{\mathrm{r}} - U - M_{\mathrm{r}}^{\mathrm{B}}$. Hence, as can be observed, the data rates are decreased due to time division, but the DL and UL transmissions in the half-duplex scheme do not suffer from any form of interference. Furthermore, no degrees-of-freedom are lost due to having to null the receive antennas. The backhaul data rates in half-duplex mode can then be expressed as

$$\begin{aligned} R^{\mathrm{u,B}} &= \sum_{k=1}^{M_{\mathrm{t}}^{\mathrm{B}}} \eta \log_2 \left(1 + \mathit{SINR}_{\mathrm{B}}^{\mathrm{u,HD}}\right) \\ &= \eta M_{\mathrm{t}}^{\mathrm{B}} \log_2 \left(1 + \frac{\Lambda_{\mathrm{t}}^{\mathrm{HD}} L_{\mathrm{B}} P_{\mathrm{u}}^{\mathrm{B}}}{M_{\mathrm{t}}^{\mathrm{B}} \sigma_{\mathrm{n}}^2}\right), \end{aligned} \tag{16}$$

$$\begin{aligned} R^{\mathrm{d,B}} &= \sum_{l=1}^{M_{\mathrm{r}}^{\mathrm{B}}} (1-\eta) \log_2 \left(1 + \mathit{SINR}_{\mathrm{B}}^{\mathrm{d,HD}}\right) \\ &= (1-\eta) M_{\mathrm{r}}^{\mathrm{B}} \log_2 \left(1 + \frac{\Lambda_{\mathrm{r}}^{\mathrm{HD}} L_{\mathrm{B}} P_{\mathrm{d}}^{\mathrm{B}}}{M_{\mathrm{r}}^{\mathrm{B}} \sigma_{\mathrm{n}}^2}\right). \end{aligned} \tag{17}$$

Based on (14)–(17), an intuitive interpretation regarding the relationship between the data rates of the full-duplex and half-duplex schemes is that it highly depends on the level of the total interference. With low path loss between the UL and DL UEs and/or poor SI cancellation performance, the half-duplex scheme is likely to be the better option due to it being immune to the interference. On the other hand, if the AN is capable of efficiently suppressing the SI signal and the UEs do not strongly interfere with each other or with the BN, the full-duplex scheme will likely provide the higher performance. These aspects are investigated further in Section V with the help of numerical results.

C. Hybrid Relay Scheme

In addition to the above extreme cases of purely full-duplex and half-duplex systems, an interesting scheme is a full-duplex relay-type AN, which simply relays the UL signal to the BN during one time slot, and then in the other time slot relays the signal from the BN to the DL UEs. The bottom part of Fig. 1 illustrates this type of a solution. The benefit of this scheme is that the problem of UL-to-DL IUI is completely avoided, similar to the half-duplex scheme, while the full-duplex capability of the AN is still utilized to some extent as the relaying is performed inband. The obvious drawback is, however, that now everything cannot be done simultaneously, which will inherently decrease the achievable rate. Furthermore, the relay scheme still suffers from the interference between the BN and the UEs.

Also the SINRs of this type of a hybrid relay scheme can be derived in a similar manner as those of the full-duplex scheme in Section II-A, the DL sum-rate being now

$$\begin{aligned} R^{\mathrm{d}} &= \sum_{i=1}^{D} R_i^{\mathrm{d}}, \\ R_i^{\mathrm{d}} &= \eta \log_2 \left(1 + \mathit{SINR}_i^{\mathrm{d,RL}}\right) \\ &= \eta \log_2 \left(1 + \frac{\Lambda_{\mathrm{t}}^{\mathrm{RL}} L_i^{\mathrm{d}} p_i^{\mathrm{d}}}{\sigma_{\mathrm{n}}^2 + L_i^{\mathrm{Bd}} P_{\mathrm{d}}^{\mathrm{B}}}\right), \end{aligned} \tag{18}$$

where $\Lambda_{\mathrm{t}}^{\mathrm{RL}} = N_{\mathrm{t}} - D - N_{\mathrm{r}}$. The UL sum-rate can correspondingly be written as:

$$\begin{aligned} R^{\mathrm{u}} &= \sum_{j=1}^{U} R_j^{\mathrm{u}}, \\ R_j^{\mathrm{u}} &= (1-\eta) \log_2 \left(1 + \mathit{SINR}_j^{\mathrm{u,RL}}\right) \\ &= (1-\eta) \log_2 \left(1 + \frac{\Lambda_{\mathrm{r}}^{\mathrm{RL}} L_j^{\mathrm{u}} p_j^{\mathrm{u}}}{\sigma_{\mathrm{n}}^2 + \alpha_{\mathrm{AN}} P_{\mathrm{u}}^{\mathrm{B}}}\right), \end{aligned} \tag{19}$$

where $\Lambda_{\mathrm{r}}^{\mathrm{RL}} = N_{\mathrm{r}} - U$. Now, there is still some interference, which degrades the DL and UL SINRs, but this scheme can be considered a trade-off between tolerating interference and duplexing the transmissions and receptions in time.

Finally, the backhaul data rates of the hybrid relay scheme can be expressed as follows:

$$\begin{aligned} R^{\mathrm{u,B}} &= \sum_{k=1}^{M_{\mathrm{t}}^{\mathrm{B}}} (1-\eta) \log_2 \left(1 + \mathit{SINR}_{\mathrm{B}}^{\mathrm{u,RL}}\right) \\ &= (1-\eta) M_{\mathrm{t}}^{\mathrm{B}} \log_2 \left(1 + \frac{\Lambda_{\mathrm{t,B}}^{\mathrm{RL}} L_{\mathrm{B}} P_{\mathrm{u}}^{\mathrm{B}} / M_{\mathrm{t}}^{\mathrm{B}}}{\sigma_{\mathrm{n}}^2 + \sum_{j=1}^{U} L_j^{\mathrm{Bu}} p_j^{\mathrm{u}}}\right), \end{aligned} \tag{20}$$

$$R^{\mathrm{d,B}} = \sum_{l=1}^{M_{\mathrm{r}}^{\mathrm{B}}} \eta \log_2\left(1 + \mathit{SINR}_{\mathrm{B}}^{\mathrm{d,RL}}\right) = \eta M_{\mathrm{r}}^{\mathrm{B}} \log_2\left(1 + \frac{\Lambda_{\mathrm{r,B}}^{\mathrm{RL}} L_{\mathrm{B}} P_{\mathrm{d}}^{\mathrm{B}}/M_{\mathrm{r}}^{\mathrm{B}}}{\sigma_{\mathrm{n}}^2 + \alpha_{\mathrm{AN}} \sum_{i=1}^{D} p_i^{\mathrm{d}}}\right), \quad (21)$$

where $\Lambda_{\mathrm{t,B}}^{\mathrm{RL}} = N_{\mathrm{t}} - N_{\mathrm{r}} - M_{\mathrm{t}}^{\mathrm{B}}$ and $\Lambda_{\mathrm{r,B}}^{\mathrm{RL}} = N_{\mathrm{r}} - M_{\mathrm{r}}^{\mathrm{B}}$ are the degrees-of-freedom of the AN transmitter and receiver for backhauling data in the hybrid relay scheme, respectively. Again, a crucial aspect of the considered cell is that the backhaul link should be able to match the data rates of UL and DL. Otherwise the system will be bottlenecked by the backhaul connection.

III. Transmit Sum-Power Minimization under Rate Constraints

Next, the problem of minimizing the transmit powers of the system under some given data rate requirements for the DL and the UL is investigated. In particular, let us define the per-UE QoS requirements in terms of the minimum data rates as ρ_{d} and ρ_{u} for the DL and the UL, respectively. This results in the following optimization problem.

Problem (Transmit Sum-Power Minimization):

$$\begin{aligned} \underset{\mathbf{p},\, P_{\mathrm{d}}^{\mathrm{B}},\, P_{\mathrm{u}}^{\mathrm{B}}}{\text{minimize}} \quad & \left(\mathbf{1}_{D+U}^T \mathbf{p} + P_{\mathrm{d}}^{\mathrm{B}} + P_{\mathrm{u}}^{\mathrm{B}}\right) \\ \text{subject to} \quad & \text{C1: } R_i^{\mathrm{d}} \geq \rho_{\mathrm{d}},\ i = 1, \ldots, D, \\ & \text{C2: } R_j^{\mathrm{u}} \geq \rho_{\mathrm{u}},\ j = 1, \ldots, U, \\ & \text{C3: } R^{\mathrm{d,B}} \geq \sum_{i=1}^{D} R_i^{\mathrm{d}}, \\ & \text{C4: } R^{\mathrm{u,B}} \geq \sum_{j=1}^{U} R_j^{\mathrm{u}}, \end{aligned} \quad (22)$$

where $\mathbf{p} = \begin{bmatrix}\mathbf{p}_{\mathrm{d}}^T & \mathbf{p}_{\mathrm{u}}^T\end{bmatrix}^T$, $\mathbf{p}_{\mathrm{d}}$ and $\mathbf{p}_{\mathrm{u}}$ are column vectors containing the DL and UL transmit powers p_i^{d} and p_j^{u} stacked, respectively, and $\mathbf{1}_N$ is a column vector consisting of N ones. The constraints C1 and C2 ensure the QoS of the UEs, while the constraints C3 and C4 ensure sufficient backhauling capability in the AN. This optimization problem will next be solved separately for the three considered communication schemes, while the associated infeasible system scenarios and QoS requirements that manifest themselves as negative transmit power values in the following theorems are characterized later in Section IV.

A. Full-Duplex Scheme

Theorem 1: The optimal DL and UL transmit powers for the full-duplex scheme are

$$\mathbf{p}^* = \begin{bmatrix}\mathbf{p}_{\mathrm{d}}^* \\ \mathbf{p}_{\mathrm{u}}^*\end{bmatrix} = \begin{bmatrix} \frac{\sigma_{\mathrm{n}}^2 \gamma_{\mathrm{d}}}{\alpha_{\mathrm{AN}}} \mathbf{q}_{\mathrm{d}} + \frac{\sigma_{\mathrm{n}}^2 \left(\frac{1+S_{\mathrm{d}}\gamma_{\mathrm{d}}}{\alpha_{\mathrm{AN}}} + \gamma_{\mathrm{t}}^{\mathrm{B}}\right)}{\theta(1-\gamma^{\mathrm{B}})} \left(\gamma_{\mathrm{d}} \gamma_{\mathrm{r}}^{\mathrm{B}} \mathbf{q}_{\mathrm{B/d}} + \frac{\gamma_{\mathrm{d}}\gamma_{\mathrm{u}}}{\alpha_{\mathrm{AN}}} \mathbf{L}_{\mathrm{ud}}^{\mathrm{d}} \mathbf{q}_{\mathrm{u}}\right) \\ \frac{\sigma_{\mathrm{n}}^2 \gamma_{\mathrm{u}} \left(\frac{1+S_{\mathrm{d}}\gamma_{\mathrm{d}}}{\alpha_{\mathrm{AN}}} + \gamma_{\mathrm{t}}^{\mathrm{B}}\right)}{\theta(1-\gamma^{\mathrm{B}})} \mathbf{q}_{\mathrm{u}} \end{bmatrix}, \quad (23)$$

when each element of $\mathbf{p}^*$ is positive and finite. Otherwise the QoS requirements cannot be fulfilled and the system is infeasible. Here, $\gamma_{\mathrm{d}} = \frac{\alpha_{\mathrm{AN}}(2^{\rho_{\mathrm{d}}}-1)}{\Lambda_{\mathrm{t}}^{\mathrm{FD}}}$, $\gamma_{\mathrm{u}} = \frac{\alpha_{\mathrm{AN}}(2^{\rho_{\mathrm{u}}}-1)}{\Lambda_{\mathrm{r}}^{\mathrm{FD}}}$, $\gamma_{\mathrm{r}}^{\mathrm{B}} = \frac{M_{\mathrm{r}}^{\mathrm{B}}\left(2^{D\rho_{\mathrm{d}}/M_{\mathrm{r}}^{\mathrm{B}}}-1\right)}{\Lambda_{\mathrm{r}}^{\mathrm{FD}} L_{\mathrm{B}}}$, $\gamma_{\mathrm{t}}^{\mathrm{B}} = \frac{M_{\mathrm{t}}^{\mathrm{B}}\left(2^{U\rho_{\mathrm{u}}/M_{\mathrm{t}}^{\mathrm{B}}}-1\right)}{\Lambda_{\mathrm{t}}^{\mathrm{FD}} L_{\mathrm{B}}}$, $\gamma^{\mathrm{B}} = \alpha_{\mathrm{AN}}\alpha_{\mathrm{BN}}\gamma_{\mathrm{t}}^{\mathrm{B}}\gamma_{\mathrm{r}}^{\mathrm{B}}$, $\{\mathbf{q}_{\mathrm{d}}\}_i = 1/L_i^{\mathrm{d}}$, $\{\mathbf{q}_{\mathrm{u}}\}_j = 1/L_j^{\mathrm{u}}$, $\{\mathbf{q}_{\mathrm{B/d}}\}_i = L_i^{\mathrm{Bd}}/L_i^{\mathrm{d}}$, $\{\mathbf{L}_{\mathrm{Bu}}\}_j = L_j^{\mathrm{Bu}}$, $\{\mathbf{L}_{\mathrm{ud}}\}_{ij} = L_{ij}^{\mathrm{ud}}$, $\mathbf{L}_{\mathrm{ud}}^{\mathrm{d}} = \mathbf{L}_{\mathrm{ud}} \circ \mathbf{q}_{\mathrm{d}} \mathbf{1}_{\mathbf{U}}^T$, and $\circ$ denotes the Hadamard product. Note that $\mathbf{q}_{\mathrm{d}}$, $\mathbf{q}_{\mathrm{u}}$, $\mathbf{q}_{\mathrm{B/d}}$, and $\mathbf{L}_{\mathrm{Bu}}$ are column vectors. Furthermore, the parameter θ is defined as

$$\theta = 1 - \frac{\gamma_{\mathrm{d}}\gamma_{\mathrm{r}}^{\mathrm{B}} S_{\mathrm{B/d}}}{1-\gamma^{\mathrm{B}}} - \frac{\gamma_{\mathrm{u}}\gamma_{\mathrm{t}}^{\mathrm{B}} S_{\mathrm{B/u}}}{1-\gamma^{\mathrm{B}}} - \frac{\gamma_{\mathrm{d}}\gamma_{\mathrm{u}} S_{\mathrm{ud}}}{\alpha_{\mathrm{AN}}(1-\gamma^{\mathrm{B}})}, \quad (24)$$

where $S_{\mathrm{d}} = \mathbf{1}_D^T \mathbf{q}_{\mathrm{d}}$, $S_{\mathrm{B/d}} = \mathbf{1}_D^T \mathbf{q}_{\mathrm{B/d}}$, $S_{\mathrm{B/u}} = \mathbf{L}_{\mathrm{Bu}}^T \mathbf{q}_{\mathrm{u}}$, and $S_{\mathrm{ud}} = \mathbf{1}_D^T \mathbf{L}_{\mathrm{ud}}^{\mathrm{d}} \mathbf{q}_{\mathrm{u}}$. The optimal backhauling powers $P_{\mathrm{d}}^{\mathrm{B}^*}$ and $P_{\mathrm{u}}^{\mathrm{B}^*}$ then follow directly from $\mathbf{p}^*$ as shown below, viz. (29), (30).

Proof: In order to arrive at the above closed-form solution, let us first rewrite Constraints C1 and C2 from (22) in terms of the individual UL and DL transmit powers as follows:

$$p_i^{\mathrm{d}} \geq \frac{(2^{\rho_{\mathrm{d}}}-1)\left(\sigma_{\mathrm{n}}^2 + L_i^{\mathrm{Bd}} P_{\mathrm{d}}^{\mathrm{B}} + \sum_{j=1}^{U} L_{ij}^{\mathrm{ud}} p_j^{\mathrm{u}}\right)}{\Lambda_{\mathrm{t}}^{\mathrm{FD}} L_i^{\mathrm{d}}}, \quad (25)$$

$$p_j^{\mathrm{u}} \geq \frac{(2^{\rho_{\mathrm{u}}}-1)\left(\sigma_{\mathrm{n}}^2 + \alpha_{\mathrm{AN}}\left[P_{\mathrm{u}}^{\mathrm{B}} + \sum_{i=1}^{D} p_i^{\mathrm{d}}\right]\right)}{\Lambda_{\mathrm{r}}^{\mathrm{FD}} L_j^{\mathrm{u}}}. \quad (26)$$

Minimizing p_i^{d} and p_j^{u} by setting them equal to their lower bounds, we can write $R_i^{\mathrm{d}} = \rho_{\mathrm{d}}\ \forall i$ and $R_j^{\mathrm{u}} = \rho_{\mathrm{u}}\ \forall j$. Hence, the backhauling constraints become $R^{\mathrm{d,B}} \geq D\rho_{\mathrm{d}}$ and $R^{\mathrm{u,B}} \geq U\rho_{\mathrm{u}}$. Utilizing (12) and (13), the following lower bounds for the backhaul-related transmit powers are obtained:

$$P_{\mathrm{d}}^{\mathrm{B}} \geq \gamma_{\mathrm{r}}^{\mathrm{B}}\left[\sigma_{\mathrm{n}}^2 + \alpha_{\mathrm{AN}}\left(P_{\mathrm{u}}^{\mathrm{B}} + \sum_{i=1}^{D} p_i^{\mathrm{d}}\right)\right], \quad (27)$$

$$P_{\mathrm{u}}^{\mathrm{B}} \geq \gamma_{\mathrm{t}}^{\mathrm{B}}\left(\sigma_{\mathrm{n}}^2 + \alpha_{\mathrm{BN}} P_{\mathrm{d}}^{\mathrm{B}} + \sum_{j=1}^{U} L_j^{\mathrm{Bu}} p_j^{\mathrm{u}}\right). \quad (28)$$

These transmit powers are also minimized by setting them equal to their lower bounds. Solving then for $P_{\mathrm{d}}^{\mathrm{B}}$ and $P_{\mathrm{u}}^{\mathrm{B}}$ in terms of p_i^{d} and p_j^{u} from (27) and (28), we get:

$$P_{\mathrm{d}}^{\mathrm{B}} = \frac{\alpha_{\mathrm{AN}}\gamma_{\mathrm{r}}^{\mathrm{B}}}{1-\gamma^{\mathrm{B}}} \sum_{i=1}^{D} p_i^{\mathrm{d}} + \frac{\alpha_{\mathrm{AN}}\gamma_{\mathrm{t}}^{\mathrm{B}}\gamma_{\mathrm{r}}^{\mathrm{B}}}{1-\gamma^{\mathrm{B}}} \sum_{j=1}^{U} L_j^{\mathrm{Bu}} p_j^{\mathrm{u}} + \frac{\left(1+\alpha_{\mathrm{AN}}\gamma_{\mathrm{t}}^{\mathrm{B}}\right)\gamma_{\mathrm{r}}^{\mathrm{B}}\sigma_{\mathrm{n}}^2}{1-\gamma^{\mathrm{B}}}, \quad (29)$$

$$P_{\mathrm{u}}^{\mathrm{B}} = \frac{\gamma^{\mathrm{B}}}{1-\gamma^{\mathrm{B}}} \sum_{i=1}^{D} p_i^{\mathrm{d}} + \frac{\gamma_{\mathrm{t}}^{\mathrm{B}}}{1-\gamma^{\mathrm{B}}} \sum_{j=1}^{U} L_j^{\mathrm{Bu}} p_j^{\mathrm{u}} + \frac{\left(1+\alpha_{\mathrm{BN}}\gamma_{\mathrm{r}}^{\mathrm{B}}\right)\gamma_{\mathrm{t}}^{\mathrm{B}}\sigma_{\mathrm{n}}^2}{1-\gamma^{\mathrm{B}}}. \quad (30)$$

Then, by substituting (29) into (25) and (30) into (26), we get the following system of $D+U$ equations with $D+U$ unknown transmit powers:

$$\mathbf{W}_{\mathrm{FD}} \mathbf{p} = \mathbf{v}_{\mathrm{FD}}, \quad (31)$$

where, by denoting a $N \times N$ identity matrix by $\mathbf{I}_N$, $\mathbf{W}_{\mathrm{FD}}$ can be written in blockwise form as

$$\mathbf{W}_{\mathrm{FD}} = \begin{bmatrix} \mathbf{I}_D - \frac{\gamma_{\mathrm{d}}\gamma_{\mathrm{r}}^{\mathrm{B}}\mathbf{q}_{\mathrm{B/d}}\mathbf{1}_D^T}{1-\gamma^{\mathrm{B}}} & -\frac{\gamma_{\mathrm{r}}^{\mathrm{B}}\gamma_{\mathrm{t}}^{\mathrm{B}}\gamma_{\mathrm{d}}\mathbf{q}_{\mathrm{B/d}}\mathbf{L}_{\mathrm{Bu}}^T}{1-\gamma^{\mathrm{B}}} - \frac{\gamma_{\mathrm{d}}\mathbf{L}_{\mathrm{ud}}^{\mathrm{d}}}{\alpha_{\mathrm{AN}}} \\ -\frac{\gamma_{\mathrm{u}}\mathbf{q}_{\mathrm{u}}\mathbf{1}_D^T}{1-\gamma^{\mathrm{B}}} & \mathbf{I}_U - \frac{\gamma_{\mathrm{u}}\gamma_{\mathrm{t}}^{\mathrm{B}}\mathbf{q}_{\mathrm{u}}\mathbf{L}_{\mathrm{Bu}}^T}{1-\gamma^{\mathrm{B}}} \end{bmatrix}, \tag{32}$$

while the vector $\mathbf{v}_{\mathrm{FD}}$ is defined as follows:

$$\mathbf{v}_{\mathrm{FD}} = \begin{bmatrix} \frac{\gamma_{\mathrm{d}}\sigma_{\mathrm{n}}^2}{\alpha_{\mathrm{AN}}}\mathbf{q}_{\mathrm{d}} + \frac{\gamma_{\mathrm{d}}\gamma_{\mathrm{r}}^{\mathrm{B}}\sigma_{\mathrm{n}}^2}{1-\gamma^{\mathrm{B}}}\left(\frac{1}{\alpha_{\mathrm{AN}}} + \gamma_{\mathrm{t}}^{\mathrm{B}}\right)\mathbf{q}_{\mathrm{B/d}} \\ \frac{\gamma_{\mathrm{u}}\sigma_{\mathrm{n}}^2}{1-\gamma^{\mathrm{B}}}\left(\frac{1}{\alpha_{\mathrm{AN}}} + \gamma_{\mathrm{t}}^{\mathrm{B}}\right)\mathbf{q}_{\mathrm{u}} \end{bmatrix}. \tag{33}$$

The solution to (31) can then simply be obtained by

$$\mathbf{p}^* = \mathbf{W}_{\mathrm{FD}}^{-1}\mathbf{v}_{\mathrm{FD}}. \tag{34}$$

To express the inverse of the matrix $\mathbf{W}_{\mathrm{FD}}$, let us first write it as a sum of three matrices as follows:

$$\mathbf{W}_{\mathrm{FD}} = \mathbf{I}_{D+U} + \mathbf{F}\mathbf{G} + \mathbf{H}, \tag{35}$$

where

$$\mathbf{F} = \begin{bmatrix} -\frac{\gamma_{\mathrm{d}}\gamma_{\mathrm{r}}^{\mathrm{B}}}{1-\gamma^{\mathrm{B}}}\mathbf{q}_{\mathrm{B/d}} & -\frac{\gamma_{\mathrm{r}}^{\mathrm{B}}\gamma_{\mathrm{t}}^{\mathrm{B}}\gamma_{\mathrm{d}}}{1-\gamma^{\mathrm{B}}}\mathbf{q}_{\mathrm{B/d}} \\ -\frac{\gamma_{\mathrm{u}}}{1-\gamma^{\mathrm{B}}}\mathbf{q}_{\mathrm{u}} & -\frac{\gamma_{\mathrm{u}}\gamma_{\mathrm{t}}^{\mathrm{B}}}{1-\gamma^{\mathrm{B}}}\mathbf{q}_{\mathrm{u}} \end{bmatrix}$$

$$\mathbf{G} = \begin{bmatrix} \mathbf{1}_D^T & \mathbf{0}_U^T \\ \mathbf{0}_D^T & \mathbf{L}_{\mathrm{Bu}}^T \end{bmatrix}$$

$$\mathbf{H} = \begin{bmatrix} \mathbf{0}_{D\times D} & -\frac{\gamma_{\mathrm{d}}}{\alpha_{\mathrm{AN}}}\mathbf{L}_{\mathrm{ud}}^{\mathrm{d}} \\ \mathbf{0}_{U\times D} & \mathbf{0}_{U\times U} \end{bmatrix}.$$

Here, $\mathbf{0}_N$ refers to a column vector consisting of N zeros, while $\mathbf{0}_{M\times N}$ refers to an $M \times N$ matrix consisting of all zeros. Now, the inverse can be written as follows:

$$\begin{aligned} \mathbf{W}_{\mathrm{FD}}^{-1} &= (\mathbf{I}_{D+U} + \mathbf{H} + \mathbf{F}\mathbf{G})^{-1} \\ &= (\mathbf{I}_{D+U} + \mathbf{H})^{-1} - (\mathbf{I}_{D+U} + \mathbf{H})^{-1}\mathbf{F} \\ &\times \left(\mathbf{I}_2 + \mathbf{G}\,(\mathbf{I}_{D+U} + \mathbf{H})^{-1}\mathbf{F}\right)^{-1}\mathbf{G}\,(\mathbf{I}_{D+U} + \mathbf{H})^{-1}, \end{aligned} \tag{36}$$

where the latter form is obtained using the Kailath Variant [43]. The inverse of the matrix $\mathbf{I}_{D+U} + \mathbf{H}$ can easily be obtained as:

$$\begin{aligned} (\mathbf{I}_{D+U} + \mathbf{H})^{-1} &= \begin{bmatrix} \mathbf{I}_{D\times D} & -\frac{\gamma_{\mathrm{d}}}{\alpha_{\mathrm{AN}}}\mathbf{L}_{\mathrm{ud}}^{\mathrm{d}} \\ \mathbf{0}_{U\times D} & \mathbf{I}_{U\times U} \end{bmatrix}^{-1} \\ &= \begin{bmatrix} \mathbf{I}_{D\times D} & \frac{\gamma_{\mathrm{d}}}{\alpha_{\mathrm{AN}}}\mathbf{L}_{\mathrm{ud}}^{\mathrm{d}} \\ \mathbf{0}_{U\times D} & \mathbf{I}_{U\times U} \end{bmatrix}. \end{aligned}$$

Furthermore, since $\mathbf{I}_2 + \mathbf{G}\,(\mathbf{I}_{D+U} + \mathbf{H})^{-1}\mathbf{F}$ is in fact a 2×2 matrix, its inverse can also be calculated in a straightforward manner. In particular, we get

$$\begin{aligned} &\left(\mathbf{I}_2 + \mathbf{G}\,(\mathbf{I}_{D+U} + \mathbf{H})^{-1}\mathbf{F}\right)^{-1} \\ &= \frac{1}{\theta}\begin{bmatrix} 1 - \frac{\gamma_{\mathrm{u}}\gamma_{\mathrm{t}}^{\mathrm{B}}\mathbf{L}_{\mathrm{Bu}}^T\mathbf{q}_{\mathrm{u}}}{1-\gamma^{\mathrm{B}}} & \frac{\gamma_{\mathrm{r}}^{\mathrm{B}}\gamma_{\mathrm{t}}^{\mathrm{B}}\gamma_{\mathrm{d}}\mathbf{1}_D^T\mathbf{q}_{\mathrm{B/d}}}{1-\gamma^{\mathrm{B}}} + \frac{\gamma_{\mathrm{d}}\gamma_{\mathrm{u}}\gamma_{\mathrm{t}}^{\mathrm{B}}\mathbf{1}_D^T\mathbf{L}_{\mathrm{ud}}^{\mathrm{d}}\mathbf{q}_{\mathrm{u}}}{\alpha_{\mathrm{AN}}(1-\gamma^{\mathrm{B}})} \\ \frac{\gamma_{\mathrm{u}}\mathbf{L}_{\mathrm{Bu}}^T\mathbf{q}_{\mathrm{u}}}{1-\gamma^{\mathrm{B}}} & 1 - \frac{\gamma_{\mathrm{d}}\gamma_{\mathrm{r}}^{\mathrm{B}}\mathbf{1}_D^T\mathbf{q}_{\mathrm{B/d}}}{1-\gamma^{\mathrm{B}}} - \frac{\gamma_{\mathrm{d}}\gamma_{\mathrm{u}}\mathbf{1}_D^T\mathbf{L}_{\mathrm{ud}}^{\mathrm{d}}\mathbf{q}_{\mathrm{u}}}{\alpha_{\mathrm{AN}}(1-\gamma^{\mathrm{B}})} \end{bmatrix}, \end{aligned}$$

where θ is the determinant of the inverted 2×2 matrix, and it is defined as shown in (24).

Having now calculated all the inverses in (36), the optimal transmit powers can be expressed by using only vector/matrix-multiplications as follows:

$$\begin{aligned} \mathbf{p}^* = \Big[&(\mathbf{I}_{D+U} + \mathbf{H})^{-1} - (\mathbf{I}_{D+U} + \mathbf{H})^{-1} \\ &\times \mathbf{F}\left(\mathbf{I}_2 + \mathbf{G}\,(\mathbf{I}_{D+U} + \mathbf{H})^{-1}\mathbf{F}\right)^{-1}\mathbf{G}\,(\mathbf{I}_{D+U} + \mathbf{H})^{-1}\Big]\mathbf{v}_{\mathrm{FD}}, \end{aligned}$$

which, after substituting the matrices with the corresponding expressions and manipulating the equation, results in (23). These DL and UL transmit powers can then be substituted into (29) and (30) in order to obtain the corresponding optimal backhaul-related transmit powers. ■

B. Half-Duplex Scheme

Theorem 2: For the half-duplex scheme, the optimal transmit powers in closed form are

$$\mathbf{p}^* = \begin{bmatrix} \mathbf{p}_{\mathrm{d}}^* \\ \mathbf{p}_{\mathrm{u}}^* \end{bmatrix} = \begin{bmatrix} \frac{\left(2^{\frac{\rho_{\mathrm{d}}}{\eta}} - 1\right)\sigma_{\mathrm{n}}^2}{\Lambda_{\mathrm{t}}^{\mathrm{HD}}}\mathbf{q}_{\mathrm{d}} \\ \frac{\left(2^{\frac{\rho_{\mathrm{u}}}{1-\eta}} - 1\right)\sigma_{\mathrm{n}}^2}{\Lambda_{\mathrm{r}}^{\mathrm{HD}}}\mathbf{q}_{\mathrm{u}} \end{bmatrix}, \tag{37}$$

$$P_{\mathrm{d}}^{\mathrm{B}^*} = \frac{\left(2^{\frac{D\rho_{\mathrm{d}}}{M_{\mathrm{r}}^{\mathrm{B}}(1-\eta)}} - 1\right)M_{\mathrm{r}}^{\mathrm{B}}\sigma_{\mathrm{n}}^2}{\Lambda_{\mathrm{r}}^{\mathrm{HD}}L_{\mathrm{B}}}, \tag{38}$$

$$P_{\mathrm{u}}^{\mathrm{B}^*} = \frac{\left(2^{\frac{U\rho_{\mathrm{u}}}{M_{\mathrm{t}}^{\mathrm{B}}\eta}} - 1\right)M_{\mathrm{t}}^{\mathrm{B}}\sigma_{\mathrm{n}}^2}{\Lambda_{\mathrm{t}}^{\mathrm{HD}}L_{\mathrm{B}}}. \tag{39}$$

The QoS requirements can always be fulfilled and the system is always feasible.

Proof: This analytical solution is again obtained by first rewriting the Constraints C1 and C2 in terms of the DL and UL transmit powers with the help of (14) and (15) as follows:

$$p_i^{\mathrm{d}} \geq \frac{\left(2^{\frac{\rho_{\mathrm{d}}}{\eta}} - 1\right)\sigma_{\mathrm{n}}^2}{\Lambda_{\mathrm{t}}^{\mathrm{HD}}L_i^{\mathrm{d}}}, \tag{40}$$

$$p_j^{\mathrm{u}} \geq \frac{\left(2^{\frac{\rho_{\mathrm{u}}}{1-\eta}} - 1\right)\sigma_{\mathrm{n}}^2}{\Lambda_{\mathrm{r}}^{\mathrm{HD}}L_j^{\mathrm{u}}}. \tag{41}$$

Again, these transmit powers are minimized by setting them equal to the lower bounds, and consequently the backhauling requirements become $R^{\mathrm{d,B}} \geq D\rho_{\mathrm{d}}$ and $R^{\mathrm{u,B}} \geq U\rho_{\mathrm{u}}$. These, together with (16) and (17), yield the following bounds for the backhaul-related transmit powers:

$$P_{\mathrm{d}}^{\mathrm{B}} \geq \frac{\left(2^{\frac{D\rho_{\mathrm{d}}}{M_{\mathrm{r}}^{\mathrm{B}}(1-\eta)}} - 1\right)M_{\mathrm{r}}^{\mathrm{B}}\sigma_{\mathrm{n}}^2}{\Lambda_{\mathrm{r}}^{\mathrm{HD}}L_{\mathrm{B}}}, \tag{42}$$

$$P_{\mathrm{u}}^{\mathrm{B}} \geq \frac{\left(2^{\frac{U\rho_{\mathrm{u}}}{M_{\mathrm{t}}^{\mathrm{B}}\eta}} - 1\right)M_{\mathrm{t}}^{\mathrm{B}}\sigma_{\mathrm{n}}^2}{\Lambda_{\mathrm{t}}^{\mathrm{HD}}L_{\mathrm{B}}}, \tag{43}$$

which are also minimized by setting them equal to their respective lower bounds. ■

Optimizing the Duplexing Parameter for the Half-duplex Scheme: In addition, for the half-duplex scheme, also the duplexing parameter η should be optimized, since it directly affects the overall transmit power. Having solved the optimal transmit powers as shown above, they can be used to formulate the optimization problem in terms of η as follows:

$$\underset{\eta}{\text{minimize}}\; S^{\mathrm{HD}}(\eta)\,, \text{ where } S^{\mathrm{HD}}(\eta) = \mathbf{1}_{D+U}^T\mathbf{p}^* + P_{\mathrm{d}}^{\mathrm{B}^*} + P_{\mathrm{u}}^{\mathrm{B}^*}. \tag{44}$$

Using (37)–(39), the objective function can be written as follows:

$$S^{\mathrm{HD}}(\eta) = \frac{\left(2^{\frac{\rho_{\mathrm{d}}}{\eta}}-1\right)\sigma_{\mathrm{n}}^2 S_{\mathrm{d}}}{\Lambda_{\mathrm{t}}^{\mathrm{HD}}} + \frac{\left(2^{\frac{\rho_{\mathrm{u}}}{1-\eta}}-1\right)\sigma_{\mathrm{n}}^2 S_{\mathrm{u}}}{\Lambda_{\mathrm{r}}^{\mathrm{HD}}} + \frac{\left(2^{\frac{D\rho_{\mathrm{d}}}{M_{\mathrm{r}}^{\mathrm{B}}(1-\eta)}}-1\right)M_{\mathrm{r}}^{\mathrm{B}}\sigma_{\mathrm{n}}^2}{\Lambda_{\mathrm{r}}^{\mathrm{HD}}L_{\mathrm{B}}} + \frac{\left(2^{\frac{U\rho_{\mathrm{u}}}{M_{\mathrm{t}}^{\mathrm{B}}\eta}}-1\right)M_{\mathrm{t}}^{\mathrm{B}}\sigma_{\mathrm{n}}^2}{\Lambda_{\mathrm{t}}^{\mathrm{HD}}L_{\mathrm{B}}},$$

where $S_{\mathrm{u}} = \mathbf{1}_U^T\mathbf{q}_{\mathrm{u}}$. It is easy to show that this is a convex function in terms of η, and hence its global minimum is found at the zero-point of its derivative. Hence, (44) is in fact equivalent to solving the following equation:

$$\begin{aligned}&\frac{\mathrm{d}}{\mathrm{d}\eta}S^{\mathrm{HD}}(\eta)\\ &= \ln(2)\,\sigma_{\mathrm{n}}^2\left(-\left(\frac{S_{\mathrm{d}}\rho_{\mathrm{d}}}{\Lambda_{\mathrm{t}}^{\mathrm{HD}}}\right)\frac{2^{\frac{\rho_{\mathrm{d}}}{\eta}}}{\eta^2} + \left(\frac{S_{\mathrm{u}}\rho_{\mathrm{u}}}{\Lambda_{\mathrm{r}}^{\mathrm{HD}}}\right)\frac{2^{\frac{\rho_{\mathrm{u}}}{1-\eta}}}{(1-\eta)^2}\right.\\ &\left.+\left(\frac{D\rho_{\mathrm{d}}}{\Lambda_{\mathrm{r}}^{\mathrm{HD}}L_{\mathrm{B}}}\right)\frac{2^{\frac{D\rho_{\mathrm{d}}}{M_{\mathrm{r}}^{\mathrm{B}}(1-\eta)}}}{(1-\eta)^2} - \left(\frac{U\rho_{\mathrm{u}}}{\Lambda_{\mathrm{t}}^{\mathrm{HD}}L_{\mathrm{B}}}\right)\frac{2^{\frac{U\rho_{\mathrm{u}}}{M_{\mathrm{t}}^{\mathrm{B}}\eta}}}{\eta^2}\right) = 0.\end{aligned} \tag{45}$$

In principle, this can be interpreted as the joint optimization problem for the transmit powers and the duplexing parameter. Namely, as the objective function in (44) is constructed from the closed-form solutions of the minimum transmit powers, which represent the optimal solution for any given duplexing parameter, substituting the optimal value of η into the expressions in (37)–(39) gives directly the transmit power allocations that have been optimized with respect to all the parameters. However, as can be easily observed, the optimal duplexing parameter does not have a closed-form solution and therefore it is solved numerically for the results of Section V.

C. Hybrid Relay Scheme

Theorem 3: The optimal DL and UL transmit powers for the hybrid relay scheme are

$$\mathbf{p}^* = \begin{bmatrix}\mathbf{p}_{\mathrm{d}}^*\\ \mathbf{p}_{\mathrm{u}}^*\end{bmatrix} = \begin{bmatrix}\frac{\gamma_{\mathrm{d}}\sigma_{\mathrm{n}}^2}{\alpha_{\mathrm{AN}}}\left(\mathbf{q}_{\mathrm{d}} + \frac{\gamma_{\mathrm{r}}^{\mathrm{B}}(1+S_{\mathrm{d}}\gamma_{\mathrm{d}})}{1-\gamma_{\mathrm{d}}\gamma_{\mathrm{r}}^{\mathrm{B}}S_{\mathrm{B/d}}}\mathbf{q}_{\mathrm{B/d}}\right)\\ \frac{\sigma_{\mathrm{n}}^2\gamma_{\mathrm{u}}}{\alpha_{\mathrm{AN}}}\left(\frac{1+\alpha_{\mathrm{AN}}\gamma_{\mathrm{t}}^{\mathrm{B}}}{1-\gamma_{\mathrm{u}}\gamma_{\mathrm{t}}^{\mathrm{B}}S_{\mathrm{B/u}}}\mathbf{q}_{\mathrm{u}}\right)\end{bmatrix}, \tag{46}$$

when each element of $\mathbf{p}^*$ is positive and finite. Otherwise the QoS requirements cannot be fulfilled and the system is infeasible. Here, $\gamma_{\mathrm{d}} = \alpha_{\mathrm{AN}}\left(\frac{2^{\rho_{\mathrm{d}}/\eta}-1}{\Lambda_{\mathrm{t}}^{\mathrm{RL}}}\right)$, $\gamma_{\mathrm{u}} = \alpha_{\mathrm{AN}}\left(\frac{2^{\rho_{\mathrm{u}}/(1-\eta)}-1}{\Lambda_{\mathrm{r}}^{\mathrm{RL}}}\right)$, $\gamma_{\mathrm{r}}^{\mathrm{B}} = M_{\mathrm{r}}^{\mathrm{B}}\left(\frac{2^{D\rho_{\mathrm{d}}/(M_{\mathrm{r}}^{\mathrm{B}}\eta)}-1}{\Lambda_{\mathrm{r,B}}^{\mathrm{RL}}L_{\mathrm{B}}}\right)$, and $\gamma_{\mathrm{t}}^{\mathrm{B}} = M_{\mathrm{t}}^{\mathrm{B}}\left(\frac{2^{U\rho_{\mathrm{u}}/(M_{\mathrm{t}}^{\mathrm{B}}(1-\eta))}-1}{\Lambda_{\mathrm{t,B}}^{\mathrm{RL}}L_{\mathrm{B}}}\right)$. The optimal backhaul-related transmit powers again directly follow from $\mathbf{p}^*$ as shown below, viz. (49), (50) with equalities.

Proof: Following a similar procedure as in the full-duplex and half-duplex schemes, the first step in obtaining the above closed-form solution is rewriting the QoS constraints in (22) as boundaries for the DL and UL transmit powers using (18) and (19) as follows:

$$p_i^{\mathrm{d}} \geq \frac{\left(2^{\frac{\rho_{\mathrm{d}}}{\eta}}-1\right)\left(\sigma_{\mathrm{n}}^2 + L_i^{\mathrm{Bd}}P_{\mathrm{d}}^{\mathrm{B}}\right)}{\Lambda_{\mathrm{t}}^{\mathrm{RL}}L_i^{\mathrm{d}}}, \tag{47}$$

$$p_j^{\mathrm{u}} \geq \frac{\left(2^{\frac{\rho_{\mathrm{u}}}{1-\eta}}-1\right)\left(\sigma_{\mathrm{n}}^2 + \alpha_{\mathrm{AN}}P_{\mathrm{u}}^{\mathrm{B}}\right)}{\Lambda_{\mathrm{r}}^{\mathrm{RL}}L_j^{\mathrm{u}}}. \tag{48}$$

Minimizing again these transmit powers by setting them equal to their lower bounds, the self-backhauling constraints become $R^{\mathrm{d,B}} \geq D\rho_{\mathrm{d}}$ and $R^{\mathrm{u,B}} \geq U\rho_{\mathrm{u}}$. Hence, by using (20) and (21), we can write:

$$P_{\mathrm{d}}^{\mathrm{B}} \geq \gamma_{\mathrm{r}}^{\mathrm{B}}\left(\sigma_{\mathrm{n}}^2 + \alpha_{\mathrm{AN}}\sum_{i=1}^{D}p_i^{\mathrm{d}}\right), \tag{49}$$

$$P_{\mathrm{u}}^{\mathrm{B}} \geq \gamma_{\mathrm{t}}^{\mathrm{B}}\left(\sigma_{\mathrm{n}}^2 + \sum_{j=1}^{U}L_j^{\mathrm{Bu}}p_j^{\mathrm{u}}\right). \tag{50}$$

Setting also these backhaul-related transmit powers equal to their lower bounds and substituting them into (47) and (48), we obtain the following expressions for the individual transmit powers:

$$p_i^{\mathrm{d}} = \frac{\gamma_{\mathrm{d}}\gamma_{\mathrm{r}}^{\mathrm{B}}L_i^{\mathrm{Bd}}}{L_i^{\mathrm{d}}}\sum_{k=1}^{D}p_k^{\mathrm{d}} + \frac{\sigma_{\mathrm{n}}^2\gamma_{\mathrm{d}}}{\alpha_{\mathrm{AN}}L_i^{\mathrm{d}}}\left(1 + L_i^{\mathrm{Bd}}\gamma_{\mathrm{r}}^{\mathrm{B}}\right), \tag{51}$$

$$p_j^{\mathrm{u}} = \frac{\gamma_{\mathrm{u}}\gamma_{\mathrm{t}}^{\mathrm{B}}}{L_j^{\mathrm{u}}}\sum_{l=1}^{U}L_l^{\mathrm{Bu}}p_l^{\mathrm{u}} + \frac{\sigma_{\mathrm{n}}^2\gamma_{\mathrm{u}}}{\alpha_{\mathrm{AN}}L_j^{\mathrm{u}}}\left(1 + \alpha_{\mathrm{AN}}\gamma_{\mathrm{t}}^{\mathrm{B}}\right). \tag{52}$$

These can easily be rearranged into a system of equations for the unknown DL and UL transmit powers as follows:

$$\mathbf{W}_{\mathrm{RL}}\mathbf{p} = \mathbf{v}_{\mathrm{RL}}, \tag{53}$$

where $\mathbf{W}_{\mathrm{RL}}$ can be written in blockwise form as

$$\mathbf{W}_{\mathrm{RL}} = \begin{bmatrix}\mathbf{I}_D - \gamma_{\mathrm{d}}\gamma_{\mathrm{r}}^{\mathrm{B}}\mathbf{q}_{\mathrm{B/d}}\mathbf{1}_D^T & \mathbf{0}_{D\times U}\\ \mathbf{0}_{U\times D} & \mathbf{I}_U - \gamma_{\mathrm{u}}\gamma_{\mathrm{t}}^{\mathrm{B}}\mathbf{q}_{\mathrm{u}}\mathbf{L}_{\mathrm{Bu}}^T\end{bmatrix}, \tag{54}$$

and the vector $\mathbf{v}_{\mathrm{RL}}$ is defined as follows:

$$\mathbf{v}_{\mathrm{RL}} = \begin{bmatrix}\frac{\sigma_{\mathrm{n}}^2\gamma_{\mathrm{d}}}{\alpha_{\mathrm{AN}}}\left(\mathbf{q}_{\mathrm{d}} + \gamma_{\mathrm{r}}^{\mathrm{B}}\mathbf{q}_{\mathrm{B/d}}\right)\\ \frac{\sigma_{\mathrm{n}}^2\gamma_{\mathrm{u}}}{\alpha_{\mathrm{AN}}}\left(1 + \alpha_{\mathrm{AN}}\gamma_{\mathrm{t}}^{\mathrm{B}}\right)\mathbf{q}_{\mathrm{u}}\end{bmatrix}. \tag{55}$$

The optimal transmit powers are then obtained similar to the full-duplex scheme, i.e., from

$$\mathbf{p}^* = \mathbf{W}_{\mathrm{RL}}^{-1}\mathbf{v}_{\mathrm{RL}}, \tag{56}$$

which, due to the block diagonal nature of the matrix $\mathbf{W}_{\mathrm{RL}}$, can in fact be solved separately for the DL and UL transmit powers. Hence, the optimal DL transmit powers are as follows:

$$\begin{aligned}\mathbf{p}_{\mathrm{d}}^* &= \left(\mathbf{I}_D - \gamma_{\mathrm{d}}\gamma_{\mathrm{r}}^{\mathrm{B}}\mathbf{q}_{\mathrm{B/d}}\mathbf{1}_D^T\right)^{-1}\frac{\sigma_{\mathrm{n}}^2\gamma_{\mathrm{d}}}{\alpha_{\mathrm{AN}}}\left(\mathbf{q}_{\mathrm{d}} + \gamma_{\mathrm{r}}^{\mathrm{B}}\mathbf{q}_{\mathrm{B/d}}\right)\\ &= \left(\mathbf{I}_D + \frac{\gamma_{\mathrm{d}}\gamma_{\mathrm{r}}^{\mathrm{B}}\mathbf{q}_{\mathrm{B/d}}\mathbf{1}_D^T}{1-\gamma_{\mathrm{d}}\gamma_{\mathrm{r}}^{\mathrm{B}}\mathbf{1}_D^T\mathbf{q}_{\mathrm{B/d}}}\right)\frac{\sigma_{\mathrm{n}}^2\gamma_{\mathrm{d}}}{\alpha_{\mathrm{AN}}}\left(\mathbf{q}_{\mathrm{d}} + \gamma_{\mathrm{r}}^{\mathrm{B}}\mathbf{q}_{\mathrm{B/d}}\right)\\ &= \frac{\sigma_{\mathrm{n}}^2\gamma_{\mathrm{d}}}{\alpha_{\mathrm{AN}}}\left(\mathbf{q}_{\mathrm{d}} + \frac{\gamma_{\mathrm{r}}^{\mathrm{B}}\left(1+S_{\mathrm{d}}\gamma_{\mathrm{d}}\right)}{1-\gamma_{\mathrm{d}}\gamma_{\mathrm{r}}^{\mathrm{B}}S_{\mathrm{B/d}}}\mathbf{q}_{\mathrm{B/d}}\right),\end{aligned} \tag{57}$$

where the matrix inverse has been calculated by using the Sherman-Morrison formula [43]. The optimal UL transmit powers are obtained in an identical manner, and they read:

$$\begin{aligned}\mathbf{p}_{\mathrm{u}}^{*} &= \left(\mathbf{I}_{U} - \gamma_{\mathrm{u}}\gamma_{\mathrm{t}}^{\mathrm{B}}\mathbf{q}_{\mathrm{u}}\mathbf{L}_{\mathrm{Bu}}^{T}\right)^{-1}\frac{\sigma_{\mathrm{n}}^{2}\gamma_{\mathrm{u}}}{\alpha_{\mathrm{AN}}}\left(1+\alpha_{\mathrm{AN}}\gamma_{\mathrm{t}}^{\mathrm{B}}\right)\mathbf{q}_{\mathrm{u}} \\ &= \frac{\sigma_{\mathrm{n}}^{2}\gamma_{\mathrm{u}}}{\alpha_{\mathrm{AN}}}\left(\frac{1+\alpha_{\mathrm{AN}}\gamma_{\mathrm{t}}^{\mathrm{B}}}{1-\gamma_{\mathrm{u}}\gamma_{\mathrm{t}}^{\mathrm{B}}S_{\mathrm{B/u}}}\mathbf{q}_{\mathrm{u}}\right). \end{aligned} \tag{58}$$

The optimal backhaul-related transmit powers can be solved by substituting the optimal DL and UL transmit powers into the expressions in (49) and (50) with equalities. ■

Optimizing the Duplexing Parameter for the Hybrid Relay Scheme: Similar to the half-duplex scheme, the solution in (56) is for a given duplexing parameter η, and thus the transmit powers of the hybrid relay scheme should be further minimized also with respect to η. This results in the following optimization problem:

$$\underset{\eta}{\text{minimize}}\; S^{\mathrm{RL}}(\eta)\,, \text{ where } S^{\mathrm{RL}}(\eta) = \mathbf{1}_{D+U}^{T}\mathbf{p}^{*} + P_{\mathrm{d}}^{\mathrm{B}^{*}} + P_{\mathrm{u}}^{\mathrm{B}^{*}}. \tag{59}$$

In order to obtain the expression of the objective function, the overall DL transmit power can first be written as follows, based on (57):

$$\begin{aligned}\mathbf{1}_{D}^{T}\mathbf{p}_{\mathrm{d}}^{*} &= \frac{\sigma_{\mathrm{n}}^{2}\gamma_{\mathrm{d}}}{\alpha_{\mathrm{AN}}}\left(\mathbf{1}_{D}^{T}\mathbf{q}_{\mathrm{d}} + \frac{\gamma_{\mathrm{r}}^{\mathrm{B}}\left(1+S_{\mathrm{d}}\gamma_{\mathrm{d}}\right)}{1-\gamma_{\mathrm{d}}\gamma_{\mathrm{r}}^{\mathrm{B}}S_{\mathrm{B/d}}}\mathbf{1}_{D}^{T}\mathbf{q}_{\mathrm{B/d}}\right) \\ &= \frac{\sigma_{\mathrm{n}}^{2}\gamma_{\mathrm{d}}}{\alpha_{\mathrm{AN}}}\left(\frac{S_{\mathrm{d}}+\gamma_{\mathrm{r}}^{\mathrm{B}}S_{\mathrm{B/d}}}{1-\gamma_{\mathrm{d}}\gamma_{\mathrm{r}}^{\mathrm{B}}S_{\mathrm{B/d}}}\right). \end{aligned} \tag{60}$$

Following a similar procedure, the sum UL transmit power is obtained using (58) as follows:

$$\mathbf{1}_{U}^{T}\mathbf{p}_{\mathrm{u}}^{*} = \frac{\sigma_{\mathrm{n}}^{2}\gamma_{\mathrm{u}}}{\alpha_{\mathrm{AN}}}\left(\frac{S_{\mathrm{u}}\left(1+\alpha_{\mathrm{AN}}\gamma_{\mathrm{t}}^{\mathrm{B}}\right)}{1-\gamma_{\mathrm{u}}\gamma_{\mathrm{t}}^{\mathrm{B}}S_{\mathrm{B/u}}}\right). \tag{61}$$

Furthermore, in order to express the transmit power used for backhauling the uplink data ($P_{\mathrm{u}}^{\mathrm{B}^{*}}$), the term $\mathbf{L}_{\mathrm{Bu}}^{T}\mathbf{p}_{\mathrm{u}}^{*}$ must be calculated. Using an identical procedure as in (61), it can be derived as follows:

$$\mathbf{L}_{\mathrm{Bu}}^{T}\mathbf{p}_{\mathrm{u}}^{*} = \frac{\sigma_{\mathrm{n}}^{2}\gamma_{\mathrm{u}}}{\alpha_{\mathrm{AN}}}\left(\frac{S_{\mathrm{B/u}}\left(1+\alpha_{\mathrm{AN}}\gamma_{\mathrm{t}}^{\mathrm{B}}\right)}{1-\gamma_{\mathrm{u}}\gamma_{\mathrm{t}}^{\mathrm{B}}S_{\mathrm{B/u}}}\right). \tag{62}$$

Having obtained the expressions for the sum DL and UL transmit powers, as well as for $\mathbf{L}_{\mathrm{Bu}}^{T}\mathbf{p}_{\mathrm{u}}^{*}$, they can be substituted into the expressions in (49) and (50) to solve the corresponding backhaul-related transmit powers. After this, the objective function can be written as follows:

$$\begin{aligned}S^{\mathrm{RL}}(\eta) = &\frac{\sigma_{\mathrm{n}}^{2}\gamma_{\mathrm{d}}\left(\alpha_{\mathrm{AN}}^{-1}+\gamma_{\mathrm{r}}^{\mathrm{B}}\right)\left(S_{\mathrm{d}}+\gamma_{\mathrm{r}}^{\mathrm{B}}S_{\mathrm{B/d}}\right)}{1-\gamma_{\mathrm{d}}\gamma_{\mathrm{r}}^{\mathrm{B}}S_{\mathrm{B/d}}} + \gamma_{\mathrm{r}}^{\mathrm{B}}\sigma_{\mathrm{n}}^{2} \\ &+ \frac{\sigma_{\mathrm{n}}^{2}\gamma_{\mathrm{u}}\left(\alpha_{\mathrm{AN}}^{-1}+\gamma_{\mathrm{t}}^{\mathrm{B}}\right)\left(S_{\mathrm{u}}+\gamma_{\mathrm{t}}^{\mathrm{B}}S_{\mathrm{B/u}}\right)}{1-\gamma_{\mathrm{u}}\gamma_{\mathrm{t}}^{\mathrm{B}}S_{\mathrm{B/u}}} + \gamma_{\mathrm{t}}^{\mathrm{B}}\sigma_{\mathrm{n}}^{2}, \end{aligned} \tag{63}$$

where the duplexing parameter η is contained in the terms γ_{d}, γ_{u}, $\gamma_{\mathrm{r}}^{\mathrm{B}}$, and $\gamma_{\mathrm{t}}^{\mathrm{B}}$, as defined earlier. As is shown in Section IV below where the feasibility of the hybrid relay scheme is discussed in more detail, the system is in fact feasible when $1-\gamma_{\mathrm{d}}^{\mathrm{B}}\gamma_{\mathrm{r}}^{\mathrm{B}}S_{\mathrm{B/d}} > 0$ and $1-\gamma_{\mathrm{u}}^{\mathrm{B}}\gamma_{\mathrm{t}}^{\mathrm{B}}S_{\mathrm{B/u}} > 0$. Solving these inequalities in terms of η results in an open interval within which the minimum point is located, and it can be easily observed that the function $S^{\mathrm{RL}}(\eta)$ is also continuous within this interval.

The above optimization problem with respect to η can also in this case be interpreted as the joint optimization problem for the transmit powers and the duplexing parameter since the resulting optimal value of η gives directly the optimal values of the transmit powers with (46), (49), and (50). As there is again no closed-form solution for the optimal η, in the forthcoming numerical results the optimal duplexing parameter is determined by numerically optimizing (63) over the open interval defined by the feasibility conditions. This can be done by utilizing any one-dimensional optimization procedure.

IV. Feasibility Analysis of Full-Duplex and Hybrid Relay Schemes

The feasibility of the considered communication schemes can be determined by investigating the resulting required transmit powers. In particular, if their values are positive and finite, the system is capable of fulfilling the QoS requirements, while infinite or negative transmit powers in the above theorems naturally indicate that the required data rates cannot be achieved. This stems from the physical interpretation of a transmit power, which obviously cannot be negative.

The half-duplex scheme does not suffer from any interference sources, and hence it is feasible under all circumstances. In other words, it can fulfill any QoS requirements with appropriately high transmit powers. However, both the full-duplex and hybrid relay schemes have various interference sources, which result in a fundamental upper bound for the achievable data rates. We refer to this as the feasibility boundary, since it determines whether the whole system is feasible in the first place. Essentially, this means that the full-duplex and hybrid relay schemes have an upper bound for the DL and/or UL data rates, which can be expressed as follows for the kth UE:

$$R_{k}^{\mathrm{x}} \leq R_{k,\max}^{\mathrm{x}} \quad \forall p_{1}^{\mathrm{d}},\ldots,p_{D}^{\mathrm{d}},p_{1}^{\mathrm{u}},\ldots,p_{U}^{\mathrm{u}},P_{\mathrm{d}}^{\mathrm{B}},P_{\mathrm{u}}^{\mathrm{B}} \geq 0,$$

where $x = d$ and/or $x = u$. This means that, if the DL/UL data rate requirement is higher than $R_{k,\max}^{\mathrm{x}}$, the QoS requirements cannot be fulfilled for the kth UE, and consequently the system is infeasible. Note that essentially this type of a feasibility analysis considers a case where all the transmit powers tend towards infinity, meaning that the derived boundary conditions are very fundamental in nature. Hence, the corresponding feasibility limits for restricted transmit powers are somewhat stricter.

A. Feasibility of the Full-duplex Scheme

Theorem 4: The feasibility condition of the full-duplex scheme can be expressed as follows:

$$\begin{cases}\dfrac{\gamma_{\mathrm{d}}\gamma_{\mathrm{r}}^{\mathrm{B}}S_{\mathrm{B/d}}}{1-\gamma^{\mathrm{B}}} + \dfrac{\gamma_{\mathrm{u}}\gamma_{\mathrm{t}}^{\mathrm{B}}S_{\mathrm{B/u}}}{1-\gamma^{\mathrm{B}}} + \dfrac{\gamma_{\mathrm{d}}\gamma_{\mathrm{u}}S_{\mathrm{ud}}}{\alpha_{\mathrm{AN}}\left(1-\gamma^{\mathrm{B}}\right)} < 1, \\ \gamma_{\mathrm{B}} < 1, \end{cases} \tag{64}$$

where the first condition is simply $\theta > 0$ rewritten in a slightly different form.

Proof: These feasibility conditions stem from the fact that all the transmit powers in (23) are positive and finite under these conditions. In particular, if $\gamma_{\mathrm{B}} < 1$, all the terms in (23), apart from θ, are always positive. Then, when also $\theta > 0$, all the transmit powers are clearly positive and the system is feasible. It is also evident from (23) that $\theta < 0$ and $\gamma^{\mathrm{B}} < 1$ result in at least the UL transmit powers being negative, while $\gamma^{\mathrm{B}} > 1$ results in $\theta > 0$, meaning that the UL transmit powers are negative also in this case. This proves that the system is infeasible if and only if the conditions in (64) do not hold. ■

Corollary 1: For any typical system parameters, the term $\alpha_{\mathrm{AN}}\alpha_{\mathrm{BN}}$ is extremely small, meaning that usually $\theta > 0$ is a sufficient feasibility condition since $\gamma^{\mathrm{B}} \ll 1$. In fact, it can be assumed with high accuracy that $\gamma^{\mathrm{B}} \approx 0$, and the feasibility condition in terms of the physical system parameters can consequently be approximated as:

$$\alpha_{\mathrm{AN}}\left(\frac{(2^{\rho_{\mathrm{u}}}-1)(2^{\rho_{\mathrm{d}}}-1)S_{\mathrm{ud}}}{\Lambda_{\mathrm{t}}^{\mathrm{FD}}\Lambda_{\mathrm{r}}^{\mathrm{FD}}}+\frac{(2^{\rho_{\mathrm{u}}}-1)(2^{\frac{U\rho_{\mathrm{u}}}{M_{\mathrm{t}}^{\mathrm{B}}}}-1)M_{\mathrm{t}}^{\mathrm{B}}S_{\mathrm{B/u}}}{\Lambda_{\mathrm{t}}^{\mathrm{FD}}\Lambda_{\mathrm{r}}^{\mathrm{FD}}L_{\mathrm{B}}}+\frac{(2^{\rho_{\mathrm{d}}}-1)(2^{\frac{D\rho_{\mathrm{d}}}{M_{\mathrm{r}}^{\mathrm{B}}}}-1)M_{\mathrm{r}}^{\mathrm{B}}S_{\mathrm{B/d}}}{\Lambda_{\mathrm{t}}^{\mathrm{FD}}\Lambda_{\mathrm{r}}^{\mathrm{FD}}L_{\mathrm{B}}}\right)<1. \tag{65}$$

Since (65) is clearly a monotonic function of ρ_{d}, the maximum supported DL data rate requirement is obtained by solving the root of the above expression with respect to ρ_{d}. Due to the multiplications of the exponential rate terms, there is no closed-form solution for the root, even if assuming that $2^{\rho_{\mathrm{d}}}-1 \approx 2^{\rho_{\mathrm{d}}}$ and $2^{D\rho_{\mathrm{d}}/M_{\mathrm{r}}^{\mathrm{B}}}-1 \approx 2^{D\rho_{\mathrm{d}}/M_{\mathrm{r}}^{\mathrm{B}}}$. Hence, the highest feasible DL data rate requirement of the full-duplex scheme is obtained by solving the root numerically.

On the other hand, when considering the required amount of SI cancellation to make the system feasible, a closed-form solution can be easily obtained from (65). In particular, the minimum amount of required SI cancellation in decibels is as follows:

$$\begin{aligned}\alpha_{\mathrm{AN}}^{\mathrm{dB}} < {} & 10\log_{10}\left(\Lambda_{\mathrm{t}}^{\mathrm{FD}}\Lambda_{\mathrm{r}}^{\mathrm{FD}}L_{\mathrm{B}}\right)\\ & -10\log_{10}\Bigg[(2^{\rho_{\mathrm{u}}}-1)\left(2^{\frac{U\rho_{\mathrm{u}}}{M_{\mathrm{t}}^{\mathrm{B}}}}-1\right)M_{\mathrm{t}}^{\mathrm{B}}S_{\mathrm{B/u}}\\ & \quad +(2^{\rho_{\mathrm{d}}}-1)\left(2^{\frac{D\rho_{\mathrm{d}}}{M_{\mathrm{r}}^{\mathrm{B}}}}-1\right)M_{\mathrm{r}}^{\mathrm{B}}S_{\mathrm{B/d}}\\ & \quad +(2^{\rho_{\mathrm{u}}}-1)(2^{\rho_{\mathrm{d}}}-1)L_{\mathrm{B}}S_{\mathrm{ud}}\Bigg].\end{aligned} \tag{66}$$

In the numerical results, these feasibility boundaries obtained from the simplified expression in Corollary 1 are compared to the exact solutions defined in Theorem 4. The approximated boundaries are shown to be highly accurate, which means that Corollary 1 can be used to obtain reliable information regarding the feasibility of a system utilizing the full-duplex scheme.

B. Feasibility of the Hybrid Relay Scheme

Theorem 5: The hybrid relay scheme is feasible under the following conditions:

$$\begin{cases}\dfrac{\alpha_{\mathrm{AN}}\left(2^{\frac{\rho_{\mathrm{d}}}{\eta}}-1\right)\left(2^{\frac{D\rho_{\mathrm{d}}}{M_{\mathrm{r}}^{\mathrm{B}}\eta}}-1\right)M_{\mathrm{r}}^{\mathrm{B}}S_{\mathrm{B/d}}}{\Lambda_{\mathrm{r,B}}^{\mathrm{RL}}\Lambda_{\mathrm{t}}^{\mathrm{RL}}L_{\mathrm{B}}}<1,\\ \dfrac{\alpha_{\mathrm{AN}}\left(2^{\frac{\rho_{\mathrm{u}}}{1-\eta}}-1\right)\left(2^{\frac{U\rho_{\mathrm{u}}}{M_{\mathrm{t}}^{\mathrm{B}}(1-\eta)}}-1\right)M_{\mathrm{t}}^{\mathrm{B}}S_{\mathrm{B/u}}}{\Lambda_{\mathrm{t,B}}^{\mathrm{RL}}\Lambda_{\mathrm{r}}^{\mathrm{RL}}L_{\mathrm{B}}}<1,\\ 0<\eta<1.\end{cases} \tag{67}$$

Proof: These conditions are obtained by observing from (46) that all the transmit powers are positive and finite when $1-\gamma_{\mathrm{d}}^{\mathrm{B}}\gamma_{\mathrm{r}}^{\mathrm{B}}S_{\mathrm{B/d}} > 0$ and $1-\gamma_{\mathrm{u}}^{\mathrm{B}}\gamma_{\mathrm{t}}^{\mathrm{B}}S_{\mathrm{B/u}} > 0$, because all the variables themselves are positive. Furthermore, since the sum DL and UL transmit powers in (60) and (61) are negative when $1-\gamma_{\mathrm{d}}^{\mathrm{B}}\gamma_{\mathrm{r}}^{\mathrm{B}}S_{\mathrm{B/d}} < 0$ and $1-\gamma_{\mathrm{u}}^{\mathrm{B}}\gamma_{\mathrm{t}}^{\mathrm{B}}S_{\mathrm{B/u}} < 0$, (67) represents indeed the exact feasibility condition. ■

When optimizing the duplexing parameter η, these conditions can be used to determine its upper and lower bound. In particular, it can easily be shown that the first condition is monotonically decreasing with respect to η, while the second condition is monotonically increasing. Hence, the first inequality results in a lower bound for η, while the second inequality defines its upper bound. The system is then feasible if there exists a value for η which fulfills all of these inequalities.

Since it is not possible to obtain closed-form solutions for the upper and lower boundaries of η using the exact form of (67), the problem can be made analytically tractable by assuming that $\left(2^{\frac{\rho_{\mathrm{d}}}{\eta}}-1\right) \approx 2^{\frac{\rho_{\mathrm{d}}}{\eta}}$, $\left(2^{\frac{\rho_{\mathrm{u}}}{1-\eta}}-1\right) \approx 2^{\frac{\rho_{\mathrm{u}}}{1-\eta}}$, $\left(2^{\frac{D\rho_{\mathrm{d}}}{M_{\mathrm{r}}^{\mathrm{B}}\eta}}-1\right) \approx 2^{\frac{D\rho_{\mathrm{d}}}{M_{\mathrm{r}}^{\mathrm{B}}\eta}}$, and $\left(2^{\frac{U\rho_{\mathrm{u}}}{M_{\mathrm{t}}^{\mathrm{B}}(1-\eta)}}-1\right) \approx 2^{\frac{U\rho_{\mathrm{u}}}{M_{\mathrm{t}}^{\mathrm{B}}(1-\eta)}}$. This approximation is rather accurate with any reasonable rate requirements, and it represents a pessimistic estimate of the feasibility boundary, which is asymptotically approaching the true boundary when $\rho_{\mathrm{d}}, \rho_{\mathrm{u}} \to \infty$. Now, the boundaries for η can be expressed as follows:

$$\frac{\rho_{\mathrm{d}}+\frac{D\rho_{\mathrm{d}}}{M_{\mathrm{r}}^{\mathrm{B}}}}{\log_2\left(\frac{\Lambda_{\mathrm{r,B}}^{\mathrm{RL}}\Lambda_{\mathrm{t}}^{\mathrm{RL}}L_{\mathrm{B}}}{\alpha_{\mathrm{AN}}M_{\mathrm{r}}^{\mathrm{B}}S_{\mathrm{B/d}}}\right)}<\eta<1-\frac{\rho_{\mathrm{u}}+\frac{U\rho_{\mathrm{u}}}{M_{\mathrm{t}}^{\mathrm{B}}}}{\log_2\left(\frac{\Lambda_{\mathrm{r}}^{\mathrm{RL}}\Lambda_{\mathrm{t,B}}^{\mathrm{RL}}L_{\mathrm{B}}}{\alpha_{\mathrm{AN}}M_{\mathrm{t}}^{\mathrm{B}}S_{\mathrm{B/u}}}\right)}.$$

Note that we have assumed here that $\frac{\Lambda_{\mathrm{r,B}}^{\mathrm{RL}}\Lambda_{\mathrm{t}}^{\mathrm{RL}}L_{\mathrm{B}}}{\alpha_{\mathrm{AN}}M_{\mathrm{r}}^{\mathrm{B}}S_{\mathrm{B/d}}} > 1$ and $\frac{\Lambda_{\mathrm{r}}^{\mathrm{RL}}\Lambda_{\mathrm{t,B}}^{\mathrm{RL}}L_{\mathrm{B}}}{\alpha_{\mathrm{AN}}M_{\mathrm{t}}^{\mathrm{B}}S_{\mathrm{B/u}}} > 1$, since this ensures that the third condition, i.e., $0<\eta<1$, is fulfilled. Because these inequalities can be expected to hold when considering any realistic system parameters, they are not explicitly analyzed in this article.

Corollary 2: Noting that, for a feasible system, the lower bound of η must be strictly less than its upper bound, an approximative feasibility condition for the hybrid relay scheme can be expressed as

$$\frac{\rho_{\mathrm{d}}+\frac{D\rho_{\mathrm{d}}}{M_{\mathrm{r}}^{\mathrm{B}}}}{\log_2\left(\frac{\Lambda_{\mathrm{r,B}}^{\mathrm{RL}}\Lambda_{\mathrm{t}}^{\mathrm{RL}}L_{\mathrm{B}}}{\alpha_{\mathrm{AN}}M_{\mathrm{r}}^{\mathrm{B}}S_{\mathrm{B/d}}}\right)}+\frac{\rho_{\mathrm{u}}+\frac{U\rho_{\mathrm{u}}}{M_{\mathrm{t}}^{\mathrm{B}}}}{\log_2\left(\frac{\Lambda_{\mathrm{r}}^{\mathrm{RL}}\Lambda_{\mathrm{t,B}}^{\mathrm{RL}}L_{\mathrm{B}}}{\alpha_{\mathrm{AN}}M_{\mathrm{t}}^{\mathrm{B}}S_{\mathrm{B/u}}}\right)}<1. \tag{68}$$

TABLE II: The essential default system parameters. Many of the parameter values are also varied in the evaluations.

Parameter	**Value**
No. of AN TX/RX antennas ($N_{\mathrm{t}}/N_{\mathrm{r}}$)	200/100
No. of DL and UL UEs ($D = U$)	10
No. of DL/UL backhaul streams ($M_{\mathrm{r}}^{\mathrm{B}}/M_{\mathrm{t}}^{\mathrm{B}}$)	12/6
Receiver noise floor (σ_{n}^2)	-90 dBm
SI cancellation in the AN/BN ($\alpha_{\mathrm{AN}}/\alpha_{\mathrm{BN}}$)	$-120/-120$ dB
Per-UE DL/UL rate requirement ($\rho_{\mathrm{d}}/\rho_{\mathrm{u}}$)	8/2 bps/Hz
Cell radius	50 m
Distance between the AN and the BN	75 m
No. of Monte Carlo simulation runs	10 000

If the lower bound is equal to the upper bound, this means that $1-\gamma_{\mathrm{d}}^{\mathrm{B}}\gamma_{\mathrm{r}}^{\mathrm{B}}S_{\mathrm{B/d}} \approx 0$ and $1-\gamma_{\mathrm{u}}^{\mathrm{B}}\gamma_{\mathrm{t}}^{\mathrm{B}}S_{\mathrm{B/u}} \approx 0$, indicating that the required transmit powers tend to infinity, and hence this condition represents the feasibility boundary.

Using (68), we can easily derive the boundary for the DL data rate requirement with respect to the other system parameters, and it is as follows:

$$\rho_{\mathrm{d}} < \frac{\log_2\left(\frac{\Lambda_{\mathrm{r,B}}^{\mathrm{RL}}\Lambda_{\mathrm{t}}^{\mathrm{RL}}L_{\mathrm{B}}}{\alpha_{\mathrm{AN}}M_{\mathrm{r}}^{\mathrm{B}}S_{\mathrm{B/d}}}\right)}{1+\frac{D}{M_{\mathrm{r}}^{\mathrm{B}}}}\left(1-\frac{\rho_{\mathrm{u}}+\frac{U\rho_{\mathrm{u}}}{M_{\mathrm{t}}^{\mathrm{B}}}}{\log_2\left(\frac{\Lambda_{\mathrm{r}}^{\mathrm{RL}}\Lambda_{\mathrm{t,B}}^{\mathrm{RL}}L_{\mathrm{B}}}{\alpha_{\mathrm{AN}}M_{\mathrm{t}}^{\mathrm{B}}S_{\mathrm{B/u}}}\right)}\right). \tag{69}$$

The minimum requirement for SI cancellation in the AN can also be written in closed form using (68). Expressing α_{AN} in decibels, it reads as follows:

$$\begin{aligned}\alpha_{\mathrm{AN}}^{\mathrm{dB}} < {} & 5\log_{10}\left(\frac{\Lambda_{\mathrm{r}}^{\mathrm{RL}}\Lambda_{\mathrm{t}}^{\mathrm{RL}}\Lambda_{\mathrm{t,B}}^{\mathrm{RL}}\Lambda_{\mathrm{r,B}}^{\mathrm{RL}}L_{\mathrm{B}}^2}{M_{\mathrm{r}}^{\mathrm{B}}M_{\mathrm{t}}^{\mathrm{B}}S_{\mathrm{B/d}}S_{\mathrm{B/u}}}\right) \\ & - \frac{5}{\log_2(10)}\Bigg[\rho_{\mathrm{d}}+\rho_{\mathrm{u}}+\frac{D\rho_{\mathrm{d}}}{M_{\mathrm{r}}^{\mathrm{B}}}+\frac{U\rho_{\mathrm{u}}}{M_{\mathrm{t}}^{\mathrm{B}}} \\ & + \Bigg[\left(\rho_{\mathrm{d}}-\rho_{\mathrm{u}}+\frac{D\rho_{\mathrm{d}}}{M_{\mathrm{r}}^{\mathrm{B}}}-\frac{U\rho_{\mathrm{u}}}{M_{\mathrm{t}}^{\mathrm{B}}}\right. \\ & \left.+\log_2\left(\frac{\Lambda_{\mathrm{t,B}}^{\mathrm{RL}}\Lambda_{\mathrm{r}}^{\mathrm{RL}}M_{\mathrm{r}}^{\mathrm{B}}S_{\mathrm{B/d}}}{\Lambda_{\mathrm{t}}^{\mathrm{RL}}\Lambda_{\mathrm{r,B}}^{\mathrm{RL}}M_{\mathrm{t}}^{\mathrm{B}}S_{\mathrm{B/u}}}\right)\right)^2 \\ & +4\left(\rho_{\mathrm{d}}+\frac{D\rho_{\mathrm{d}}}{M_{\mathrm{r}}^{\mathrm{B}}}\right)\left(\rho_{\mathrm{u}}+\frac{U\rho_{\mathrm{u}}}{M_{\mathrm{t}}^{\mathrm{B}}}\right)\Bigg]^{1/2}\Bigg]. \end{aligned} \tag{70}$$

Note that solving (68) for α_{AN} requires solving the roots of a 2nd-degree polynomial, but one of the two solutions can easily be shown to result in the duplexing parameter being outside the open interval $(0,1)$. Hence, there is only one valid solution for the inequality. In Section V, the above feasibility boundaries given by Corollary 2 are shown to be very close to the exact feasibility boundaries given by Theorem 5. Hence, these approximative closed-form boundaries provide highly accurate results when determining the feasibility of the hybrid relay scheme.

V. Numerical Results

Next, the proposed system is numerically evaluated with Monte Carlo simulations. In particular, we consider a cell of a given size where the specified amount of DL and UL UEs are randomly positioned. By calculating the optimal transmit powers and the feasibility conditions for a large number of random positions, the cumulative distribution functions (CDFs) of the corresponding quantities can then be obtained. The default system parameters, which are used unless otherwise mentioned, are shown in Table II. The path losses between the different parties are calculated based on the distances in each random realization, using the measurement-based path loss model for a center frequency of 3.5 GHz presented in [44] to reflect a concrete practical example; the line-of-sight (LOS) model is adopted for the link between the AN and the BN, while the non-line-of-sight (NLOS) model is adopted in all the other cases. To ensure a practical system, the scheduled DL and UL UEs are chosen from the opposite sides of the cell, which results in a smaller level of UL-to-DL IUI [41]. The UEs can then alternate between DL and UL modes at regular intervals, by which each UE gets served both in the DL and in the UL, regardless of their position in the cell. Furthermore, in order to facilitate a fair comparison between the different schemes, in the forthcoming figures the transmit powers of the half-duplex and hybrid relay scheme are weighted by the proportion of time spent in the corresponding time slot (determined by the duplexing parameter η). For brevity, the full-duplex, half-duplex and hybrid relay schemes are referred to as FD, HD, and RL, respectively, in all the figures.

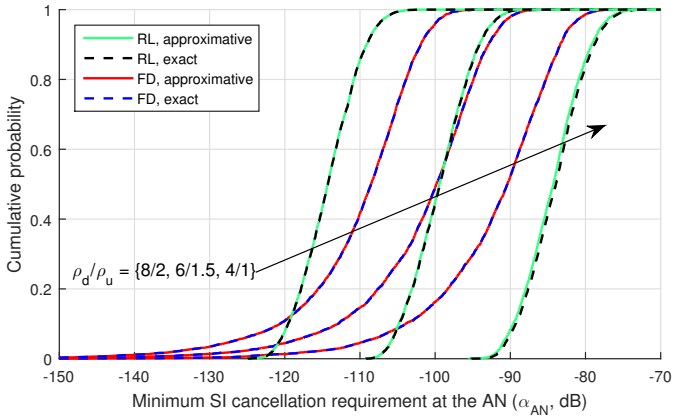

Fig. 3: CDFs of the minimum SI cancellation requirement in the AN in the full-duplex and hybrid relay schemes, shown for different DL/UL data rate requirements.

A. Feasibility

In order to first analyze the feasibility of the full-duplex and the hybrid relay schemes, Fig. 3 shows the CDFs of the SI cancellation performance required in the AN to make the system feasible. The figure shows both the approximated closed-form solutions given in (66) and (70) as well as the exact solutions obtained from (64) and (67). Firstly, it can be observed that the approximated feasibility boundaries match the exact boundaries very closely, indicating that the approximations do not compromise the accuracy of the derived equations. Furthermore, Fig. 3 indicates that the required AN SI cancellation performance of the full-duplex scheme is less affected by the data rate requirements than that of the

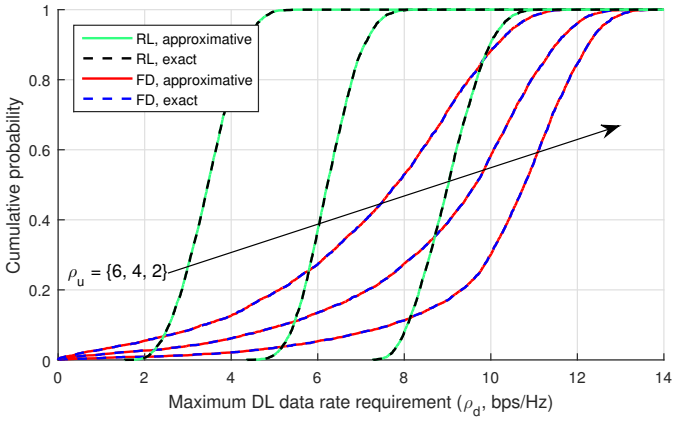

Fig. 4: CDFs of the maximum supported DL data rate requirement in the full-duplex and hybrid relay schemes, shown for different UL data rate requirements.

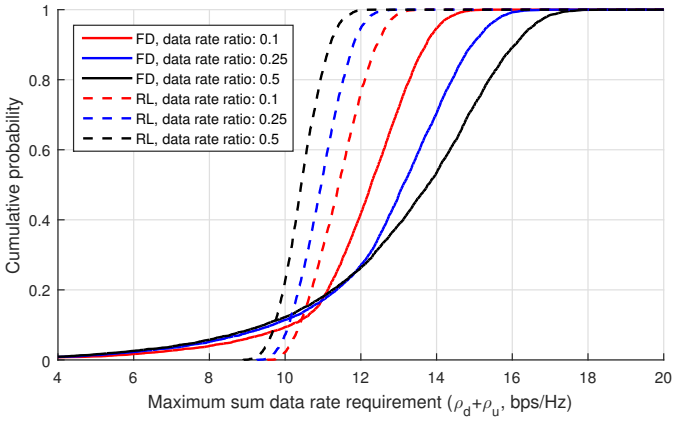

Fig. 5: CDFs of the maximum supported sum data rate requirement in the full-duplex and hybrid relay schemes under different fixed UL/DL data rate ratios.

hybrid relay scheme. In particular, with the highest data rate requirements, the full-duplex scheme is feasible with lower SI cancellation performance than the hybrid relay scheme, while the opposite is true for the lowest considered data rate requirements. In the latter case, the hybrid relay scheme benefits from the fact that it only needs to transmit to the UEs *or* to the BN, unlike the full-duplex scheme which must transmit everything at the same time. This results in less stringent SI cancellation requirements. However, with the higher data rate requirements, this benefit is overshadowed by the need to perform time-division duplexing.

Another perspective into the feasibility is the highest supported DL data rate requirement. The corresponding CDFs are plotted in Fig. 4, which again show the approximated boundaries given by (65) and (69), alongside with the exact feasibility boundaries obtained from (64) and (67). Also now, the approximated feasibility boundaries are essentially similar to the exact boundaries, further confirming their accuracy under the studied conditions. It can also be concluded that the full-duplex scheme can support a higher DL data rate requirement with all the considered UL data rate requirements. However, it should be noted that there is more uncertainty regarding the maximum supported DL data rate requirement in the full-duplex scheme, since the slope of the CDF is lower than in the hybrid relay scheme. Hence, even though the full-duplex scheme supports a higher median DL data rate requirement, there is a higher probability that it cannot fulfill that for different randomly chosen UE positions in the network. This indicates that there is a trade-off between the maximum performance and robustness when comparing the full-duplex and hybrid relay schemes.

The maximum supported sum data rate requirement is then analyzed in Fig. 5. There, the CDFs of the feasibility boundary are shown under a scenario where the ratio between the UL and DL data rates is fixed, that is, $\rho_{\mathrm{u}}/\rho_{\mathrm{d}} = c$ for some constant c. In this case, the CDFs are only shown for the approximated equations in order to make the figure more readable. In general, the full-duplex scheme supports also a higher median sum data rate requirement, although the uncertainty in the supported data rate requirement is again somewhat higher than in the hybrid relay scheme.

It can also be observed from Fig. 5 that the hybrid relay scheme supports higher sum data rate requirements with lower data rate ratios. This stems from the system parameters having been chosen to support a higher DL data rate ($M_{\mathrm{r}}^{\mathrm{B}} > M_{\mathrm{t}}^{\mathrm{B}}$) to reflect the data traffic distribution of a practical network [25], which results in the hybrid relay scheme benefiting from a DL-oriented data rate distribution. On the other hand, the full-duplex scheme seems to be better suited for a more even distribution of the DL and UL data rate requirements, which is evident from Fig. 5 when investigating the median values of the highest supported sum-rate requirements. This is due to the more symmetric nature of the full-duplex scheme since it has less options for dividing the resources between UL and DL. Hence, unlike the hybrid relay scheme, which has the benefit of a duplexing parameter, the full-duplex scheme requires a more even data rate distribution to support the highest sum-rates.

Finally, Fig. 6 shows the probability of feasibility with respect to the number of UEs in the full-duplex and hybrid relay schemes, assuming $D = U$. The probabilities have been obtained by evaluating the approximated feasibility boundaries in (65) and (68) for different numbers of UEs. Firstly, it can be observed from Fig. 6 that the full-duplex scheme can in general fulfill the QoS requirements for a larger number of randomly positioned UEs, especially when the AN is capable of efficient SI cancellation. With the lower AN SI cancellation performances, the hybrid relay scheme is more evenly matched with the full-duplex scheme, being again the more robust option in terms of fulfilling the QoS requirements. Namely, while the full-duplex scheme can in general support a larger number of UEs, the slope of the probability curve is steeper with the hybrid relay scheme, indicating that the latter is the more predictable option when there is a moderate number of UEs in the cell. This somewhat resembles the behaviour of the maximum supported DL data rate requirements in Fig. 4. Nevertheless, with sufficiently high AN SI cancellation performance, the full-duplex scheme is clearly the superior option with regard to the number of supported UEs.

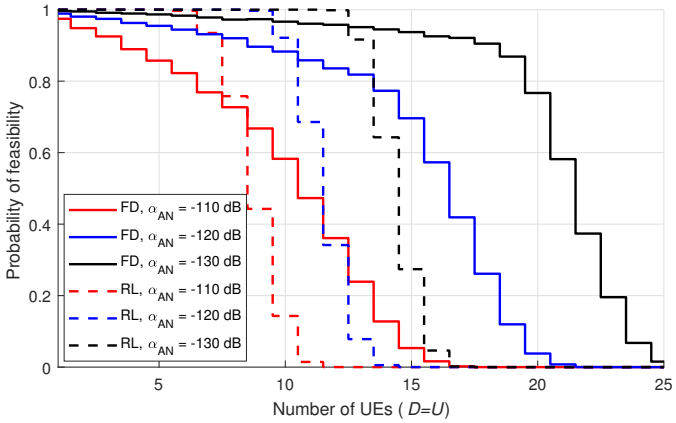

Fig. 6: The probability of feasibility with respect to the number of UEs ($U = D$) in the full-duplex and hybrid relay schemes, shown for different AN SI cancellation performances.

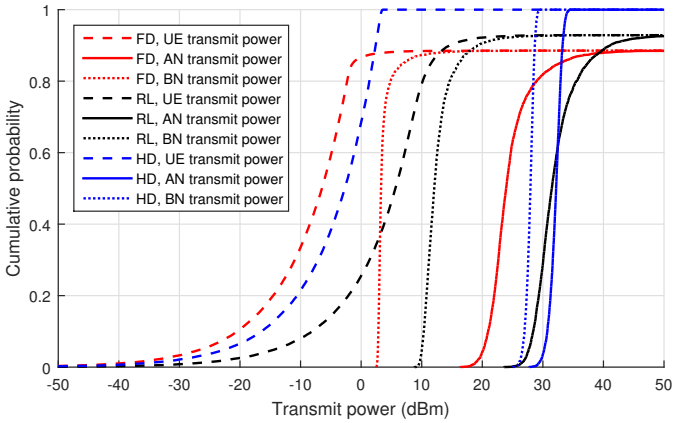

Fig. 7: CDFs of the transmit powers of the individual parties with the default system parameters.

B. Transmit Powers

To then investigate the transmit power efficiency of the different communication schemes, the CDFs of the transmit powers of the AN, each individual UE, and the BN are first shown in Fig. 7 using the default system parameters. It can be observed that the full-duplex scheme obtains the lowest transmit powers for all the communicating parties. However, the downside of the full-duplex scheme is its inability to fulfill the QoS requirements in some cases, evidenced by the fact that the CDFs saturate to a value below 1. These cases represent the situations where the feasibility conditions in (64) are not fulfilled, and therefore the highest value of the CDF is in fact the probability of feasibility of the corresponding system, illustrated also in Fig. 6 with respect to the number of UEs. This deduction is further confirmed by Fig. 3, which shows that the SI cancellation requirement is indeed more than -120 dB in some cases when $\rho_{\mathrm{d}} = 8$ and $\rho_{\mathrm{u}} = 2$.

From the perspective of the overall transmit power consumption, the hybrid relay scheme is then the next best option, while the half-duplex scheme outperforms the hybrid relay scheme in terms of minimizing the UE transmit powers. The reason for this stems from the fact that in the half-duplex scheme the UE transmissions occur in the same time slot where the DL data is backhauled. Due to the higher DL data rate requirements, this results in a somewhat longer time slot for the UE transmissions, allowing for a lower UE transmit power. Note that this occurs due to the optimal duplexing parameter being chosen by minimizing the *total transmit power*. A different outcome would be obtained if a UE-transmit-power-minimizing duplexing parameter was used. What is more, the hybrid relay scheme also suffers from the inability to fulfill the QoS requirements under some circumstances, similar to the full-duplex scheme.

To observe the effect of the SI cancellation capability of the AN, Fig. 8 shows then the CDFs of the total transmit power of the whole radio access system for different values of α_{AN}. Again, the transmit power usage of the full-duplex scheme is significantly lower than that of the other schemes, regardless of the AN SI cancellation performance. However, with the lower values of α_{AN}, the probability of fulfilling the QoS requirements with the full-duplex scheme drops rather low. This is also evident from Fig. 3, where it can clearly be seen that the SI cancellation requirement is beyond -110 dB with a large probability when $\rho_{\mathrm{d}} = 8$ and $\rho_{\mathrm{u}} = 2$. Hence, the lower probability of feasibility is the cost of the low transmit power consumption.

The hybrid relay scheme also outperforms the half-duplex scheme when α_{AN} is -120 dB or better, while it performs very poorly with the lowest considered AN SI cancellation performance. This is explained by the CDF of the SI cancellation requirement shown in Fig. 3, which indicates that the SI cancellation requirement of the hybrid relay scheme is in the majority of the cases more than -110 dB. Still, even with $\alpha_{\mathrm{AN}} = -120$ dB, the probability of the hybrid relay scheme having to use more power for the transmissions than the half-duplex scheme is rather high, suggesting that it requires relatively high SI cancellation performance in the AN in order to be a viable option.

To investigate the effect of the cell size on the different schemes, Fig. 9 shows the CDFs of the total transmit power for different cell radii. Again, with all considered cell sizes, the full-duplex scheme is the most power-efficient option, while the hybrid relay scheme and the half-duplex scheme are quite closely matched. Especially with the larger cell sizes, their median transmit power usages are nearly the same. However, the hybrid relay scheme again suffers from the fact that it cannot fulfill the QoS requirements for some UE positions and thus, regardless of the higher median power, the half-duplex scheme might be the more favorable option of these two.

On a more general note, the cell size has a rather significant impact on the required transmit power, as can be expected. For instance, the total median transmit power of the full-duplex scheme is increased by almost 20 dB when the cell radius is increased from 25 m to 75 m. Moreover, with the highest considered cell radius of 75 m, the full-duplex and the hybrid relay schemes cannot fulfill the QoS requirements for a significant portion of the UE positions. Hence, it can be concluded that especially the schemes utilizing inband full-duplex communications are best suited for relatively small cells.

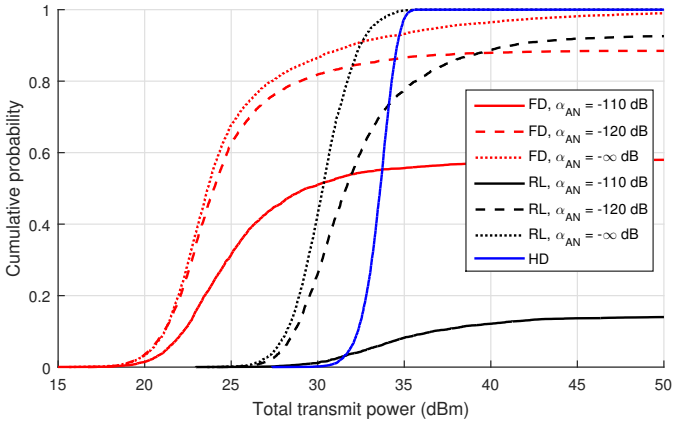

Fig. 8: CDFs of the total used transmit power of each scheme, shown for different values of SI cancellation.

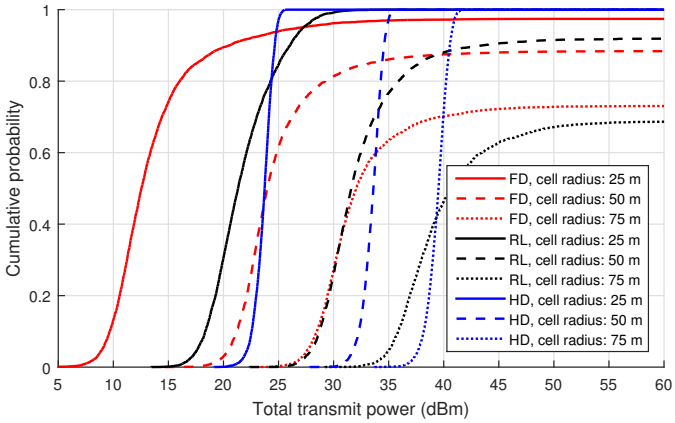

Fig. 9: CDFs of the total used transmit power of each scheme, shown for different cell radii. The distance between the AN and the BN is retained at $\frac{3}{2}$ times the cell radius.

VI. Conclusion

In this paper, we investigated a self-backhauling inband full-duplex access node with large antenna arrays, which can use the same time-frequency resource for serving the mobile users as well as for backhauling, thereby significantly reducing the cost of deployment in ultra-dense networks. Three different communication schemes for the access node were analyzed: a purely full-duplex scheme, a purely half-duplex scheme, and a hybrid scheme where the access node acts as a one-directional full-duplex relay. Especially, we derived the optimal transmit powers for the different communication schemes in closed form when a QoS requirement for each mobile user is given. In this work, QoS was defined as a minimum achievable data rate. In addition, we showed that the QoS requirements cannot always be achieved when using a full-duplex-capable access node, expressing this feasibility condition also in closed form. Evaluating then the transmit powers and feasibility conditions with realistic system parameter values, it was observed that having a purely full-duplex access node provides usually the lowest transmit powers for all communicating parties. However, the downside of the purely full-duplex scheme is its inability to fulfill the QoS requirements under some circumstances, characterized by the closed-form feasibility conditions. The numerical results also indicated that utilizing a self-backhauling full-duplex access node is best suited for relatively small cells.

References

[1] M. Duarte, C. Dick, and A. Sabharwal, "Experiment-driven characterization of full-duplex wireless systems," *IEEE Trans. Wireless Commun.*, vol. 11, no. 12, pp. 4296–4307, Dec. 2012.

[2] B. Day, A. Margetts, D. Bliss, and P. Schniter, "Full-duplex bidirectional MIMO: Achievable rates under limited dynamic range," *IEEE Trans. Signal Process.*, vol. 60, no. 7, pp. 3702–3713, Jul. 2012.

[3] D. Korpi, T. Riihonen, V. Syrjälä, L. Anttila, M. Valkama, and R. Wichman, "Full-duplex transceiver system calculations: Analysis of ADC and linearity challenges," *IEEE Trans. Wireless Commun.*, vol. 13, no. 7, pp. 3821–3836, Jul. 2014.

[4] S. Goyal, P. Liu, S. S. Panwar, R. A. Difazio, R. Yang, and E. Bala, "Full duplex cellular systems: Will doubling interference prevent doubling capacity?" *IEEE Commun. Mag.*, vol. 53, no. 5, pp. 121–127, May 2015.

[5] M. Jain, J. I. Choi, T. Kim, D. Bharadia, S. Seth, K. Srinivasan, P. Levis, S. Katti, and P. Sinha, "Practical, real-time, full duplex wireless," in *Proc. 17th Annu. Int. Conf. Mobile Comput. Netw.*, Sep. 2011, pp. 301–312.

[6] M. Heino et al., "Recent advances in antenna design and interference cancellation algorithms for in-band full-duplex relays," *IEEE Commun. Mag.*, vol. 53, no. 5, pp. 91–101, May 2015.

[7] D. Bharadia, E. McMilin, and S. Katti, "Full duplex radios," in *Proc. SIGCOMM'13*, Aug. 2013, pp. 375–386.

[8] D. Korpi, J. Tamminen, M. Turunen, T. Huusari, Y.-S. Choi, L. Anttila, S. Talwar, and M. Valkama, "Full-duplex mobile device: Pushing the limits," *IEEE Commun. Mag.*, vol. 54, no. 9, pp. 80–87, Sep. 2016.

[9] M. Mohammadi, H. A. Suraweera, Y. Cao, I. Krikidis, and C. Tellambura, "Full-duplex radio for uplink/downlink wireless access with spatially random nodes," *IEEE Trans. Commun.*, vol. 63, no. 12, pp. 5250–5266, Dec. 2015.

[10] T. Riihonen, S. Werner, and R. Wichman, "Mitigation of loopback self-interference in full-duplex MIMO relays," *IEEE Trans. Signal Process.*, vol. 59, no. 12, pp. 5983–5993, Dec. 2011.

[11] T. Riihonen, M. Vehkaperä, and R. Wichman, "Large-system analysis of rate regions in bidirectional full-duplex MIMO link: Suppression versus cancellation," in *Proc. 47th Annu. Conf. Inform. Sci. Sys.*, Mar. 2013, pp. 1–6.

[12] D. Korpi, T. Riihonen, and M. Valkama, "Achievable rate regions and self-interference channel estimation in hybrid full-duplex/half-duplex radio links," in *Proc. 47th Annu. Conf. Inform. Sci. Sys.*, Mar. 2015, pp. 1–6.

[13] D. Korpi, T. Riihonen, K. Haneda, K. Yamamoto, and M. Valkama, "Achievable transmission rates and self-interference channel estimation in hybrid full-duplex/half-duplex MIMO relaying," in *Proc. 82nd IEEE Veh. Technol. Conf.*, Sep. 2015.

[14] V. Aggarwal, M. Duarte, A. Sabharwal, and N. Shankaranarayanan, "Full- or half-duplex? A capacity analysis with bounded radio resources," in *Proc. IEEE Inform. Theory Workshop*, Sep. 2012, pp. 207–211.

[15] C. Psomas, M. Mohammadi, I. Krikidis, and H. A. Suraweera, "Impact of directionality on interference mitigation in full-duplex cellular networks," *IEEE Trans. Wireless Commun.*, vol. 16, no. 1, pp. 487–502, Jan. 2017.

[16] L. Anttila, D. Korpi, V. Syrjälä, and M. Valkama, "Cancellation of power amplifier induced nonlinear self-interference in full-duplex transceivers," in *Proc. 47th Asilomar Conf. Signals Syst. Comput.*, Nov. 2013, pp. 1193–1198.

[17] D. Korpi, L. Anttila, V. Syrjälä, and M. Valkama, "Widely linear digital self-interference cancellation in direct-conversion full-duplex transceiver," *IEEE J. Sel. Areas Commun.*, vol. 32, no. 9, pp. 1674–1687, Sep. 2014.

[18] E. Ahmed, A. M. Eltawil, and A. Sabharwal, "Self-interference cancellation with nonlinear distortion suppression for full-duplex systems," in *Proc. 47th Asilomar Conf. Signals Syst. Comput.*, Nov. 2013, pp. 1199–1203.

[19] B. Kaufman, J. Lilleberg, and B. Aazhang, "An analog baseband approach for designing full-duplex radios," in *Proc. 47th Asilomar Conf. Signals Syst. Comput.*, Nov. 2013, pp. 987–991.

[20] Y. Liu, X. Quan, W. Pan, S. Shao, and Y. Tang, "Nonlinear distortion suppression for active analog self-interference cancellers in full duplex wireless communication," in *Proc. Globecom Workshops*, Dec. 2014, pp. 948–953.

[21] J. Tamminen, M. Turunen, D. Korpi, T. Huusari, Y.-S. Choi, S. Talwar, and M. Valkama, "Digitally-controlled RF self-interference canceller for

full-duplex radios," in *Proc. Europ. Signal Process. Conf.*, Aug. 2016, pp. 783–787.
[22] A. Sabharwal, P. Schniter, D. Guo, D. Bliss, S. Rangarajan, and R. Wichman, "In-band full-duplex wireless: Challenges and opportunities," *IEEE J. Sel. Areas Commun.*, vol. 32, no. 9, Oct. 2014.
[23] E. Everett, M. Duarte, C. Dick, and A. Sabharwal, "Empowering full-duplex wireless communication by exploiting directional diversity," in *Proc. 45th Asilomar Conf. Signals Syst. Comput.*, Nov. 2011, pp. 2002–2006.
[24] D. Korpi, T. Riihonen, and M. Valkama, "Inband full-duplex radio access system with self-backhauling: Transmit power minimization under QoS requirements," in *Proc. 42nd Int. Conf. Acoust. Speech Signal Process.*, Mar. 2017, pp. 6558–6562.
[25] Nokia Solutions and Networks, "TD-LTE frame configuration primer," Nov. 2013, white paper.
[26] E. Everett and A. Sabharwal, "Spatial degrees-of-freedom in large-array full-duplex: The impact of backscattering," *EURASIP J. Wireless Commun. Netw.*, vol. 2016, no. 1, p. 286, Dec. 2016.
[27] I. Harjula, R. Wichman, K. Pajukoski, E. Lähetkangas, E. Tiirola, and O. Tirkkonen, "Full duplex relaying for local area," in *Proc. 24th Annu. IEEE Int. Symp. Personal, Indoor, and Mobile Radio Commun.*, Sep. 2013, pp. 2684–2688.
[28] R.-A. Pitaval, O. Tirkkonen, R. Wichman, K. Pajukoski, E. Lähetkangas, and E. Tiirola, "Full-duplex self-backhauling for small-cell 5G networks," *IEEE Wireless Commun.*, vol. 22, no. 5, pp. 83–89, Oct. 2015.
[29] Z. Zhang, X. Wang, K. Long, A. Vasilakos, and L. Hanzo, "Large-scale MIMO-based wireless backhaul in 5G networks," *IEEE Wireless Commun.*, vol. 22, no. 5, pp. 58–66, Oct. 2015.
[30] H. Tabassum, A. H. Sakr, and E. Hossain, "Analysis of massive MIMO-enabled downlink wireless backhauling for full-duplex small cells," *IEEE Trans. Commun.*, vol. 64, no. 6, pp. 2354–2369, Jun. 2016.
[31] S. Hong, J. Brand, J. Choi, M. Jain, J. Mehlman, S. Katti, and P. Levis, "Applications of self-interference cancellation in 5G and beyond," *IEEE Commun. Mag.*, vol. 52, no. 2, pp. 114–121, Feb. 2014.
[32] G. Chen, Y. Gong, P. Xiao, and R. Tafazolli, "Dual antenna selection in self-backhauling multiple small cell networks," *IEEE Commun. Lett.*, vol. 20, no. 8, pp. 1611–1614, Aug. 2016.
[33] D. Korpi, T. Riihonen, and M. Valkama, "Self-backhauling full-duplex access node with massive antenna arrays: Power allocation and achievable sum-rate," in *Proc. Europ. Signal Process. Conf.*, Aug. 2016, pp. 1618–1622.
[34] Nokia Solutions and Networks, "Ten key rules of 5G deployment," 2015, white paper C401-01178-WP-201503-1-EN.
[35] P. Kela, J. Turkka, and M. Costa, "Borderless mobility in 5G outdoor ultra-dense networks," *IEEE Access*, vol. 3, pp. 1462–1476, Aug. 2015.
[36] X. Huang, K. Yang, F. Wu, and S. Leng, "Power control for full-duplex relay-enhanced cellular networks with QoS guarantees," *IEEE Access*, vol. 5, pp. 4859–4869, Mar. 2017.
[37] A. Sharma, R. K. Ganti, and J. K. Milleth, "Joint backhaul-access analysis of full duplex self-backhauling heterogeneous networks," *IEEE Trans. Wireless Commun.*, vol. 16, no. 3, pp. 1727–1740, Mar. 2017.
[38] H. Q. Ngo, H. Suraweera, M. Matthaiou, and E. Larsson, "Multipair full-duplex relaying with massive arrays and linear processing," *IEEE J. Sel. Areas Commun.*, vol. 32, no. 9, pp. 1721–1737, Sep. 2014.
[39] A. Sahai, S. Diggavi, and A. Sabharwal, "On degrees-of-freedom of full-duplex uplink/downlink channel," in *Proc. IEEE Inform. Theory Workshop*, Sep. 2013, pp. 1–5.
[40] K. Kim, S. W. Jeon, and D. K. Kim, "The feasibility of interference alignment for full-duplex MIMO cellular networks," *IEEE Commun. Lett.*, vol. 19, no. 9, pp. 1500–1503, Sep. 2015.
[41] M. Duarte, A. Feki, and S. Valentin, "Inter-user interference coordination in full-duplex systems based on geographical context information," in *Proc. IEEE Int. Conf. Commun.*, May 2016, pp. 1–7.
[42] H. Yang and T. Marzetta, "Performance of conjugate and zero-forcing beamforming in large-scale antenna systems," *IEEE J. Sel. Areas Commun.*, vol. 31, no. 2, pp. 172–179, Feb. 2013.
[43] K. B. Petersen and M. S. Pedersen, "The matrix cookbook," Nov. 2012, version 20121115. [Online]. Available: http://www2.imm.dtu.dk/pubdb/p.php?3274
[44] I. Rodriguez et al., "Path loss validation for urban micro cell scenarios at 3.5 GHz compared to 1.9 GHz," in *Proc. IEEE Global Commun. Conf.*, Dec. 2013, pp. 3942–3947.

Dani Korpi (S'14–M'18) was born in Ilmajoki, Finland, in 1989. He received his M.Sc. and D.Sc. degrees (both with distinction) in communications engineering and electrical engineering from Tampere University of Technology, Finland, in 2014 and 2017, respectively. He is currently a postdoctoral researcher in the Laboratory of Electronics and Communications Engineering at the same university. So far, he has authored or co-authored 37 refereed articles and one book chapter. His current research interests include inband full-duplex radios, modeling and compensation of analog circuit impairments in radio transceivers, and 5G New Radio systems.

Taneli Riihonen (S'06–M'14) received the D.Sc. degree in electrical engineering (with distinction) from Aalto University, Finland, in August 2014. He is currently an Assistant Professor at the Laboratory of Electronics and Communications Engineering, Tampere University of Technology, Finland. He held various research positions at Helsinki University of Technology and Aalto University School of Electrical Engineering from September 2005 through December 2017. He was a Visiting Associate Research Scientist and an Adjunct Assistant Professor at Columbia University, USA, from November 2014 through December 2015. He has been nominated eleven times as an Exemplary/Top Reviewer of various IEEE journals and is serving as an Editor for IEEE COMMUNICATIONS LETTERS since October 2014 and for IEEE WIRELESS COMMUNICATIONS LETTERS since May 2017. He received the Finnish technical sector's award for the best doctoral dissertation of the year and the EURASIP Best PhD Thesis Award 2017. His research activity is focused on physical-layer OFDM(A), multiantenna, relaying and full-duplex wireless techniques with current interest in the evolution of beyond 5G systems.

Ashutosh Sabharwal (S'91–M'99–SM'06–F'14) received the B.Tech. degree from Indian Institute of Technology (IIT) Delhi, New Delhi, India, in 1993, and the M.S. and Ph.D. degrees from The Ohio State University, Columbus, OH, USA, in 1995 and 1999, respectively. He is currently a Professor with the Department of Electrical and Computer Engineering, Rice University, Houston, TX, USA. His research interests include information theory, communication algorithms, and the experiment-driven design of wireless networks. He was a recipient of the 1998 Presidential Dissertation Fellowship Award and 2017 Jack Neubauer Memorial Award.

Mikko Valkama (S'00–M'01–SM'15) was born in Pirkkala, Finland, on November 27, 1975. He received the M.Sc. and Ph.D. Degrees (both with honors) in electrical engineering (EE) from Tampere University of Technology (TUT), Finland, in 2000 and 2001, respectively. In 2002, he received the Best Ph.D. Thesis -award by the Finnish Academy of Science and Letters for his dissertation entitled "Advanced I/Q signal processing for wideband receivers: Models and algorithms". In 2003, he was working as a visiting post-doc research fellow with the Communications Systems and Signal Processing Institute at SDSU, San Diego, CA. Currently, he is a Full Professor and Laboratory Head at the Laboratory of Electronics and Communications Engineering at TUT, Finland. His general research interests include radio communications, communications signal processing, estimation and detection techniques, signal processing algorithms for flexible radios, cognitive radio, full-duplex radio, radio localization, and 5G mobile radio networks.